

*h. silberman*  
*Personal File*  
Permanent File Copy

UNIVERSITY OF MINNESOTA  
ST. ANTHONY FALLS HYDRAULIC LABORATORY

St. Anthony Falls Hydraulic Laboratory

LORENZ G. STRAUB, Director

Technical Paper No. 33, Series B

# Experimental Studies of Cavitation Noise in a Free-Jet Tunnel

by

C. S. SONG and E. SILBERMAN



July 1961

Minneapolis, Minnesota

UNIVERSITY OF MINNESOTA  
ST. ANTHONY FALLS HYDRAULIC LABORATORY  
LORENZ G. STRAUB, Director

Technical Paper No. 33, Series B

# Experimental Studies of Cavitation Noise in a Free-Jet Tunnel

by

C. S. SONG and E. SILBERMAN



July 1961

Minneapolis, Minnesota

Experimental Studies of  
Cavitation Noise in a Free-Jet Turbine

Reproduction in whole or in part is permitted  
for any purpose of the United States Government



## A B S T R A C T

The present paper summarizes the results of experimental studies on cavitation noise generated in the free-jet tunnel at St. Anthony Falls Hydraulic Laboratory in the period October 1960 to June 1961.

Two-dimensional test bodies of different shapes, such as a circular cylinder, wedge, and a Tulin-Burkhart hydrofoil were tested. Various types of cavitating flows, namely, transient cavities, steady-state cavities, and non-stationary cavities were covered. Special attention was given to the effect of ventilation on the intensity of cavitation noise. Effects of body size and the presence of a solid boundary were also investigated.

## C O N T E N T S

	Page
Abstract . . . . .	iii
List of Illustrations . . . . .	v
I. INTRODUCTION . . . . .	1
II. EXPERIMENTAL APPARATUS . . . . .	2
A. Free-Jet Tunnel . . . . .	2
B. Noise-Measuring Equipment . . . . .	3
III. EXPERIMENTAL RESULTS . . . . .	4
A. Low-Frequency Measurement . . . . .	5
1. Background Noise . . . . .	5
2. Oscillographic Records of Cavitation Noise . . . . .	6
a. Natural Cavities . . . . .	6
b. Ventilated Cavities . . . . .	7
3. Frequency Spectrum of Cavitation Noise . . . . .	7
4. Determination of the Cause of the Peaks . . . . .	9
a. Characteristics of the Pressure Transducer . . . . .	9
b. Resonance of the Test Body . . . . .	9
c. Resonance of the Water Tunnel and Ac- cessories . . . . .	10
d. Fluttering of Cavity Tail and Wake . . . . .	10
5. Some Other Factors Affecting the Low-Frequency Noise . . . . .	11
a. Scale Effect . . . . .	11
b. Wall Effect . . . . .	13
B. High-Frequency Measurement . . . . .	13
1. Oscillographic Records of Background and Cavitation Noises . . . . .	14
2. Frequency Spectrum of Cavitation Noise . . . . .	15
IV. CONCLUSION . . . . .	16
List of References . . . . .	17
Figures 1 through 22 . . . . .	21

L I S T O F I L L U S T R A T I O N S

Figure		Page
1	Background Noise Picked Up by Diaphragm-Type Transducer Mounted on Tunnel Wall . . . . .	21
2	Typical Pressure Records of Natural Cavities as Measured by Diaphragm-Type Transducer Outside of the Wake (1/2-in. Full-Span Circular Cylinder) . . . . .	22
3	Typical Pressure Records of Natural Cavities as Measured by Diaphragm-Type Transducer in the Wake (1/2-in. Full-Span Circular Cylinder) . . . . .	23
4	Typical Pressure Records of Ventilated Cavities as Measured by Diaphragm-Type Transducer (1/2-in. Full-Span Circular Cylinder) . . . . .	24
5	Response Characteristics of Hewlett Packard 300 A Harmonic Wave Analyzer and Panoramic Ultrasonic Analyzer . . . . .	25
6	Typical Frequency Spectrum of Low-Frequency Noise of Natural Cavities . . . . .	26
7	Typical Frequency Spectrum of Low-Frequency Noise of Ventilated Cavities . . . . .	27
8	Pressure Amplitude as a Function of Cavitation Number (1/2-in. Full-Span Circular Cylinder) . . . . .	28
9	Low-Frequency Measurement Using a Barium Titanate Crystal as a Pressure Transducer (1/2-in. Full-Span Circular Cylinder) . . . . .	29
10	Resonance Frequency of 1/2-in. Circular Cylinders . . . . .	30
11	Resonance Frequencies of the Water Tunnel and Accessories . . . . .	31
12	Pressure Change Due to Fluttering of Cavity Tail and Wake . . . . .	32
13	Solutions of Rayleigh's Equation of Motion for a Collapsing Spherical Bubble . . . . .	33
14	Effect of Body Size on Cavitation Noise . . . . .	33
15	Effect of a Solid Wall on Cavitation Noise Generated by a Full-Span Wedge . . . . .	34
16	Frequency Response of the Barium Titanate Crystal Transducer . . . . .	35
17	Oscillographic Records of Background Noise Picked Up by the Barium Titanate Crystal Transducer Mounted on a 1/2-in. Full-Span Circular Cylinder . . . . .	36

Figure		Page
18	Typical Oscillographic Records of Cavitation Noise Picked Up by the Barium Titanate Crystal Transducer . . . . .	37
19	Cavitation Noise Picked Up at the Front End of the Body Compared with that Picked Up at the Rear End of the Body . . . .	38
20	Typical Frequency Spectrum of Cavitation Noise at the Free-Jet Water Tunnel Compared with the Result of Mellen . . . . .	39
21	Frequency Spectra of Natural Cavities . . . . .	40
22	Frequency Spectra of Ventilated Cavities . . . . .	41

# EXPERIMENTAL STUDIES OF CAVITATION NOISE IN A FREE-JET TUNNEL

## I. INTRODUCTION

One of the phenomena pertinent to cavitation is the acoustic radiations due to the expansion and collapse of gas bubbles. In many cases the noise level may become objectionably high and it is desirable to suppress or reduce the noise level.

Customarily, cavities are classified into three categories [1]\*: transient cavities, steady-state cavities, and nonstationary cavities. Transient cavitation is an erratic process during which a large number of cavitation bubbles appear in scattered positions throughout a region under reduced pressure. It is well known that the sound source of a transient cavity is the expansion and collapse of individual gas bubbles. The steady-state cavity is a large, stationary cavity filled with a mixture of gas, water vapor, and the fluid brought into the cavity by the reentrant jet. The term "steady-state" applies only to the average shape of the cavity. Even a casual observer may note at once the roughness of the cavity boundary and the milky appearance of the cavity which involves countless numbers of gas bubbles whose motions are clearly nonstationary. The nonstationary motion of those gas bubbles is also believed to be the main source of the sound from the steady cavity. The term "nonstationary" applies to cavities resembling the steady-state cavities but whose average size and/or shape vary with time. Examples occur in the air-water entry of a missile, cavities behind an accelerating body, and cavities with varying ventilation rate. Pulsating cavities produced by ventilation [2, 3] also fall in this category. In this case, the sound energy emitted by the volume pulsation of the main cavity far exceeds that from the small bubbles.

The occurrence of individual cavitation bubbles is, in most circumstances, a random process and the contribution of each bubble to the over-all noise is very difficult to detect. However, due to the fact that the spectrum of a random sequence of similar pulses has the same form as the spectrum of a single pulse [4], a great deal about cavitation noise can be learned by studying the behavior of a single cavitation bubble, or vice versa. For this

---

\*Numbers in brackets refer to List of References on p. 17.



reason, attention has been mainly directed toward the investigation of pressure pulses produced by collapse of an empty cavity or of a gas-filled cavity. The importance of a fundamental study of this sort cannot be overemphasized. In spite of the importance of the problem and the great effort spent by many investigators, the problem still remains virtually unsolved. The increasing interest in high-speed hydrocraft designs demands immediate availability of experimental data which may be used as guides. There is considerable literature available in this regard and it will be discussed in various parts of the paper.

Some time ago, it was observed while studying ventilated cavities that cavitation noise could be reduced by introducing air into the flow at the rear end of a cavitating body. Also observed was a change of noise level while cavities change from the transient condition to the steady-cavity condition. These experiences stimulated the current interest in the cavitation noise study and led to an experimental investigation described herein. The experiments were conducted in the free-jet tunnel at the St. Anthony Falls Hydraulic Laboratory of the University of Minnesota. The present paper summarizes the experimental results and offers some explanations of the results.

This research has been supported by the Office of Naval Research of the U. S. Department of the Navy under Contract Nonr 710(24) Task NR 062-052. The entire project was under the general direction of Dr. Lorenz G. Straub, Director of the St. Anthony Falls Hydraulic Laboratory. Mr. John Almo was mainly responsible for the experimental observations and data analysis with the assistance of John Kolodnyoki and Paul Edstrom. The authors are also grateful to Messrs. John M. Killen and Frank Schiebe for their technical assistance. The manuscript was prepared for printing by Mrs. Robert Minish under the general supervision of Mr. Loyal Johnson.

## II. EXPERIMENTAL APPARATUS

### A. Free-Jet Tunnel

The experimental studies were conducted in the two-dimensional, gravity-flow, free-jet water tunnel at the St. Anthony Falls Hydraulic Laboratory. The tunnel is a free-falling, nonrecirculating type utilizing river water and having a vertical test section. The tunnel test section is designed

to produce a rectangular jet 5 in. thick between solid walls and of variable width between free surfaces. For the present experiment, a 10-in. wide jet was used exclusively. The working velocity of the jet is between 20 fps and 50 fps. Any pressure between vapor pressure and atmospheric pressure can be created at the test section. This tunnel has two principal features that make it especially useful for the type of investigation reported herein: (a) very low cavitation numbers can be obtained without blockage; and (b) large quantities of air can be added to a cavity without subsequently having to remove the air from the tunnel water. Furthermore, the test section is completely transparent, facilitating visual observation and photography. The free-jet tunnel is described in detail in Ref. [5].

The methods of velocity and ambient pressure measurement are described in detail in Refs. [2] and [5]. Water temperature was measured by a thermometer inserted into the tunnel above the test section. No attempt was made to measure the free-gas content of the water.

Test bodies are cylindrical and are mounted so as to span the 5-in. thickness of the jet between solid walls or so as to project from one of the walls half way to the other. These mountings are termed "full-span" and "half-span," respectively. Air could be introduced into a cavity region behind a body through tubes which were built into the test bodies and also through pressure taps in the rear test-section wall. The air tubes emerged from the trailing ends of the bodies and pointed downstream. Either room pressure or compressed air could be applied to the air intake. The rate of air flow was measured by a variable-area flow meter.

#### B. Noise-Measuring Equipment

Low-frequency components of the cavitation noise were measured by a diaphragm-type pressure transducer. This was a consolidated electrodynamic type 4-312A pressure pickup with a range of  $\pm 25$  psi mounted flush with the inner surface of the test-section wall. Two locations on the wall were used. The first, 5-1/2 in. downstream of the center of the test body, was used for measuring pressure variations inside a cavity or a wake, and the second, 9 in. downstream and 2 in. to one side of the test body, was used for measuring pressure variations outside a cavity.

The pickup was connected to a consolidated electrodynamic type I-127 carrier amplifier and type 5-116 recording oscillograph. This arrangement was

used for a continuous record of the pressure variations in the test section and had a frequency range of 0 to 3000 cps. Since the continuous pressure record obtained with the recording oscillograph was very complex, no frequency analysis of the pressure record was attempted. Rather, a Hewlett Packard model 300-A harmonic wave analyzer was connected to the output of the carrier amplifier and the pressure amplitudes of the individual components of the sound wave were measured.

For higher frequency measurements, a small piece of barium titanate crystal taken from a 1/2-in. diameter circular cylindrical crystal was mounted in a 1/2-in. diameter circular cylindrical test body. The crystal was a 60-degree arc measuring 3/4 in. long and 1/8 in. thick. It was carefully cemented into the test body by means of rubber cement in a slot machined to fit the crystal. The test body was installed so that it could be rotated to orient the crystal in any direction.

With some modification, the pressure variations detected by the crystal could also be recorded or analyzed by a harmonic wave analyzer. However, for the frequency range of interest, it was more convenient to use a panoramic model 5B-7bF ultrasonic analyzer. The analyzer automatically measures the frequency and amplitude of ultrasonic signals through a 200 kc range in any part of a 2 kc to 300 kc band. Direct reading of the signal was made possible by a continuous over-all graphic presentation of the spectrum on a long-persistence cathode-ray-tube screen. The graph appearing on the screen could also be photographed and analyzed later.

The crystal was calibrated against a standard hydrophone in a large tank of still water up to 150 kc frequency.

### III. EXPERIMENTAL RESULTS

It is generally agreed that the main source of cavitation noise is the expansion and collapse of individual bubbles filled with gas and water vapor. The principal variables governing the motion of the walls of a spherical bubble are (1) ambient pressure  $P_0$ , (2) original size and gas content of the bubble, (3) temperature of water, and (4) the properties of the fluid involved. Since the free-jet water tunnel utilizes river water and since no attempt was made to measure the free-gas content of the water, items (2) and

(4) were beyond control. Water temperature may play an important role in cavitation noise because the vapor pressure is a direct function of temperature. The strong effect of temperature on cavitation was clearly demonstrated in Ref. [6]. The weight loss due to cavitation pitting of a brass surface was shown to increase initially with temperature, reaching a maximum value at about 60 C, and falling sharply as temperature increases further. Fortunately, within the range of the temperature change of the present experiment, the vapor pressure was very low and erosion as predicted in [6] is nearly constant. For this reason, the temperature change was considered to be of minor importance herein.

The present experiment now reduces to the investigation of cavitation noise under different boundary conditions, that is, under varying ambient pressure  $P_0$ . Remembering that the ambient pressure  $P_0$  is a time-dependent function, one can easily see its complexity. It varies not only with the cavitating body but also with the type of cavitation. As was mentioned in the introduction, the various types of cavitation may be classified into three categories: transient cavities, steady-state cavities, and nonstationary cavities. In the subsequent part of the report, data obtained for these different types of cavitation will be presented.

#### A. Low-Frequency Measurement

Here low frequency is meant to be a frequency below 2 kilocycles per second. Any frequency above this value is regarded as a high frequency. This classification is merely for convenience in as much as different types of equipment were used for different frequency ranges. A diaphragm-type pressure transducer, as described in section II, mounted flush with the inside of the tunnel wall was used for the low-frequency pressure fluctuation measurements.

##### 1. Background Noise

Since the water tunnel is located on the main floor of the Laboratory near the machine shop, and since no special protection against outside noise is provided, the outside interference could be serious, especially when some of the shop machines are operating. Fortunately, it was soon found that the pressure transducer was very insensitive to external noise sources. Oscillographic records of pressure fluctuations for different flow conditions

without any test body in the test section are shown in Fig. 1. These records were reproducible regardless of shop activity. The gradual increase in amplitude from Fig. 1(a) to Fig. 1(c) is attributed to increase in turbulence level associated with the velocity increase of the basic flow. The sudden increase in amplitude in Fig. 1(d) is associated with the inception of cavitation around the circumference of the transducer where it joins the tunnel wall.

## 2. Oscillographic Records of Cavitation Noise

### a. Natural Cavities

Typical records of pressure oscillations produced by natural cavitation on a 1/2-in. diameter full-span circular cylinder picked up by a transducer located at 9 in. below and 2 in. to one side of the test body are shown in Fig. 2. The records are arranged in order of decreasing reference cavitation number,  $\sigma_v$ , defined as follows:

$$\sigma_v = \frac{P_\infty - P_v}{1/2\rho U^2}$$

where  $P_\infty$  is the ambient pressure and  $P_v$  is the vapor pressure.

It is readily seen that the amplitude first increases as  $\sigma_v$  decreases, reaching a plateau for a certain range of  $\sigma_v$ , and then decreases again as  $\sigma_v$  increases. Transient cavities were observed to occur in the range corresponding to the increasing noise level. On the other hand, constant cavity noise and reducing cavity noise corresponded to steady-state cavities.

Pressure records obtained in the wake may look materially different from those obtained outside the wake. Figure 3 shows typical oscillographic records obtained by a transducer located on the test section centerline 5-1/2 in. downstream from the center of the test body. The following distinct characteristics are observed: First, low-frequency, high-amplitude pressure fluctuations, presumably due to large-scale turbulence created by vortex shedding, appear even when cavitation is absent. Second, even much lower-frequency (order of 10 cps), high-amplitude fluctuations appear on the record, Fig. 3(e), when the tail of the cavity is near the pressure transducer. (Compare the 8-in. long cavities in Figs. 2 and 3.) The result of the frequency spectrum analysis discussed in section 4d below indicates that the low-frequency

pulse may be attributable to shifting of the rear stagnation point. Finally, Fig. 3(f) shows that pressure fluctuation inside the cavity is very small.

#### b. Ventilated Cavities

It is well known that ventilation raises the cavity pressure and, hence, reduces the cavitation number defined as

$$\sigma = \frac{P_{\infty} - P_c}{1/2\rho U^2}$$

where  $\sigma$  is the cavitation number and  $P_c$  is the pressure in the cavity;

One result of ventilation is a sharp reduction of low-frequency noise as demonstrated by the typical oscillographic records of Fig. 4. [The transducer was located outside of the wake for records (a) through (f) and inside for (g) and (h).] Part of the noise reduction is undoubtedly associated with cavity growth (the phenomenon shown in Fig. 2) and the remainder must be due to the presence of air. The effect of ventilation on cavitation noise will become clearer when its frequency spectrum is analyzed and discussed in the next section.

A unique phenomenon pertinent to ventilated cavities in a free jet is the pulsation of cavity shape and pressure as reported in Refs. [2] and [3]. Here, it is sufficient to note that the resulting pressure pulsation is a nearly-perfect sinusoid. Figure 4(e) is the pressure record of a steady cavity shortly before pulsation. Figure 4(f) is the pressure record of the same cavity when it pulsates. It is interesting to note that the higher-frequency, random fluctuations of Fig. 4(e) are retained in Fig. 4(f), superimposed on the pulsation. Pressure records of corresponding cavities taken inside the cavities show no high-frequency components, as may be seen in Fig. 4(g) and Fig. 4(h). There is no appreciable pressure fluctuation within a steady cavity.

Similar records obtained for a hydrofoil and other test bodies do not differ much from those of the 1/2-in. circular cylinder and will not be included in this report.

### 3. Frequency Spectrum of Cavitation Noise

To facilitate further understanding of the low-frequency noise, it was decided to carry out a frequency spectrum analysis. For this purpose, a

harmonic wave analyzer as described in section II was used. The selectivity curve of the analyzer given by the manufacturer is reproduced in Fig. 5(a). The similar curve for the high-frequency measuring equipment to be discussed later is shown in Fig. 5(b). Except where otherwise indicated, the pressure transducer was located outside of the wake and cavity.

A typical frequency spectrum for the 1/2-in. full-span circular cylinder is shown in Fig. 6(a). Here the reference cavitation number was slightly below the incipient cavitation number and the cavity was of transient type. Similar curves for a modified Tulin-Burkhart hydrofoil of 2-1/2 in. chord are shown in Fig. 6(b). Here the lowest curve is for a noncavitating condition, the middle curve is for a transient cavity, and the upper curve is for a partial steady cavity. The effect of ventilation on low-frequency noise is shown in Fig. 7. The upper graph is for variable ventilation with constant  $\sigma_v$  and the lower graph is for constant  $\sigma$ .

Curves shown in Fig. 6 and many other frequency spectrum curves for natural and ventilated cavities of full-span test bodies revealed the following common characteristics:

- (1) There are several peaks occurring in the frequency range of approximately 60 cps to 1 kcps. Those peaks are very sensitive to flow conditions. They could be so sharp that the noise was essentially harmonic, as some of the oscillographic records show in Figs. 2, 3, and 4. At some other conditions, they may be too mild to be recognized. Although the frequency analyzer is not designed for frequencies lower than 20 cps, it appears that, in all cases, there is another maximum at a frequency less than 60 cps.
- (2) In all cases, ventilation seems to reduce the sharp peaks.
- (3) As an average, discarding peaks, noise level is highest in the neighborhood of 500 cps or less, decreasing to small values as the frequency increases.

As will be discussed in the next section, most of the peaks are probably due to resonance of the test body and tunnel structure. Even though the peaks may be attributable to resonance of various kinds, it is clear that they are stimulated by the original cavitation noise and, therefore, they are some

kind of measure of the original noise. A series of tests was made for the 1/2-in. full-span circular cylinder with the specific purpose of measuring peaks. Several runs, each starting from a natural cavity and gradually increasing the cavity size by admitting air into the cavity, were made. The second peak, which occurred in the neighborhood of 150 cps, is plotted as a function of  $\sigma$  in Fig. 8(a). Open symbols indicate a natural cavity and shaded symbols indicate a ventilated cavity. Similar data for the third peak, which occurred in the neighborhood of 250 cps, are plotted in Fig. 8(b). Both figures clearly demonstrate that the peaks for natural cavities first increase, reaching a maximum point, and then decrease as the cavitation number is being decreased from that of no cavitation to that of a long steady cavity. The strong effect of ventilation is also evident. The maximum of the third peak, as shown by (b), occurs at about  $\sigma = 0.6$ , which roughly corresponds to the transition point between the transient cavity and the steady cavity. The maximum of the second peak occurs at  $\sigma = 0.4$ , which is slightly beyond the transition point. Root mean square of pressure fluctuations were also measured in this experiment and data were plotted in Fig. 8(c). Similar trends can also be seen in this figure.

#### 4. Determination of the Cause of the Peaks

##### a. Characteristics of the Pressure Transducer

According to the manufacturer's specification, the natural frequency of the transducer is 4 kcps and the frequency response below 4 kcps is very uniform. It is, therefore, considered that the peaks occurring at frequencies below 1 kcps could not be attributable to nonlinear frequency response. For the purpose of double checking, a similar low-frequency measurement was also performed by using the barium titanate crystal mounted on the test body as described in section II. A typical frequency spectrum is shown in Fig. 9(a) and the second peak is plotted in Fig. 9(b). This confirms, at least qualitatively, the earlier results.

##### b. Resonance of the Test Body

It was thought conceivable that the peaks were due to test-body resonance. To test the resonance frequency of the body, a speaker coil was attached to the 1/2-in. full-span circular cylinder and was driven by a signal generator. The electrical potential generated on the barium titanate crystal due to the vibration of the cylinder was measured. Fig. 10(a) shows the voltage output



as a function of the frequency of the exciting force when the tunnel was dry. The resonant frequency of the body is determined to be about 700 cps for this particular body. Figure 10(b) shows the result of the similar test for a half-span circular cylinder of the same diameter. By this experiment it becomes reasonably certain that the peak marked (5) in Fig. 6(a) was due to the resonance of the test body.

#### c. Resonance of the Water Tunnel and Accessories

Since there are so many parts of the tunnel and the accessories, which may vibrate separately or as a group, it is almost impossible to determine the natural frequencies of each part. The empty tunnel was first excited by applying a vibrating force to one of the pressure taps on the wall at 21 in. below the test body. The voltage output read on the barium titanate crystal on the 1/2-in. cylinder as a function of frequency for constant input voltage of 0.5 volt is plotted in Fig. 11(a). Beside the resonance of the test body at 700 cps, two sharp peaks occurred at 190 cps and 255 cps.

More revealing are the next two figures, Fig. 11(b) and Fig. 11(c), which show the effect of the excitation when the water tunnel is operating. The dotted line in Fig. 11(b) is the noise picked up by the barium titanate crystal on the 1/2-in. cylinder without excitation and the solid line in the same figure is the combined result of the original noise and that due to excitation. It is noted that the excitation nearly doubled the amplitude for all the frequency range tested. Similar data measured by the diaphragm transducer when the test body was removed from the test section, shown in Fig. 11(c), reveal the same trend. The fact that the artificial excitation of constant amplitude raised the noise level by nearly a constant factor for nearly all the frequencies tested suggests that the original noise was nearly flat and most of the peaks are due to resonance.

#### d. Fluttering of Cavity Tail and Wake

The wakes behind a body under noncavitating condition and under transient cavitation are usually unsteady. Even for a steady cavity, fluttering of the cavity tail is the rule. These two phenomena (unsteady wake and fluttering cavity tail), which are believed to be related, create oscillating pressure fields. The frequency of the oscillation is of the order of 10 cps. (See Fig. 3.)

Although the frequency of the pressure field oscillation is usually lower than the minimum operating frequency of the frequency analyzer, it was readily detected. All frequency spectrum curves such as shown in Figs. 6, 7, and 9 indicate increasing amplitude as frequency decreases below 60 cps, suggesting a possible peak at a frequency below 20 cps. The amplitude at  $f = 20$  cps is plotted as a function of cavity length in Fig. 12 for three different transducer locations. Figure 12(a) is for the case when the transducer is on the test body while Fig. 12(b) and Fig. 12(c) are for cases when the transducer is 5-1/2 in. and 9 in., respectively, below the test body. It is clearly demonstrated by these curves that the pressure amplitude is greatest when the tail of the cavity is nearest the transducer. The pressure amplitude drops as the cavity tail moves away from the transducer in both directions.

The interesting fact that this type of pressure fluctuation is not materially affected by ventilation should be noted.

## 5. Some Other Factors Affecting the Low-Frequency Noise

### a. Scale Effect

The Rayleigh equation of motion for an expanding and collapsing spherical bubble of incompressible fluid

$$R \ddot{R} + \frac{3}{2} \dot{R}^2 = \frac{P - P_{\infty}}{\rho} \quad (1)$$

may help visualization of the effect of bubble size on pressure of collapse. If it is assumed that the pressure inside the bubble is space independent, that the boundary pressure  $P_{\infty}$  is constant and that the surface tension is negligible, then the equation of motion may be written as

$$Z \ddot{Z} + \frac{3}{2} \dot{Z}^2 = C_1^2 Z^{-3\kappa} - C_2^2 \quad (2)$$

where

$$Z = \frac{R}{R_0}, \quad C_1^2 = \frac{P_0}{\rho R_0^2}, \quad C_2^2 = \frac{P_{\infty}}{\rho R_0^2}$$

$R$  = Radius of the bubble at any time  $t$

$R_0$  =  $R(t = 0)$  = Maximum radius of the bubble

$P_0$  =  $P(t = 0)$

$\kappa$  = Gas constant for adiabatic expansion

It is seen that the solution of (2) depends on two parameters,  $C_1$  and  $C_2$ . Numerical solutions of Eq. (2) for some given  $C_1$  and  $C_2$  values satisfying the initial condition

$$Z'(0) = 1, \quad \dot{Z}(0) = 0$$

are plotted in Fig. 13. It is interesting to note from the figure that the final pressure is very sensitive to  $C_1$  whereas the time of collapse is very sensitive to  $C_2$ . It is also noted that Eq. (2) may be integrated once [4] and the maximum pressure of collapse may be computed approximately as

$$\frac{P_{\max}}{P_0} = \left[ 1 + (\kappa - 1) \frac{P_{\infty}}{P_0} \right]^{\frac{\kappa}{\kappa - 1}} \quad (3)$$

It is now readily seen that when  $P_{\infty}$  is constant the maximum pressure of collapse is determined by the initial cavity pressure  $P_0$  and the time of collapse is determined by the maximum bubble size  $R_0$ . The sharp reduction of the cavitation noise due to ventilation as discussed in the earlier section is, probably, partially attributable to increasing initial pressure in the bubbles leaving the cavitation zone.

Now consider the case when cavitation bubbles originate from gas nuclei of equal sizes and gas content. If evaporation and condensation of water vapor is instantaneous so that the effect of water vapor is small, then  $P_0$  must be proportional to  $R_0^{-5}$ . This leads to the conclusion that, for a given air content, the final pressure is mainly determined by  $R_0$  and time of collapse is mainly determined by  $P_{\infty}/R_0^2$ .

An experiment of Harrison at the David Taylor Model Basin [7] revealed an almost linear relationship between maximum bubble size and the maximum radiated pressure-pulse amplitude. Scale effect on cavitation noise has also been studied by Kermeen [8]. He tested a number of spherical bodies of different sizes and found that both incipient cavitation number of transient cavities and the cavitation number corresponding to the maximum noise intensity of steady cavities are functions of body size and velocity of flow.

To supplement the findings of Harrison and Kermeen, additional data were obtained for 1/2-in. and 1/4-in. full-span circular cylinders. Only the

root mean square of the sound pressure for natural cavities was measured. In all cases the pressure transducer was 2 in. off the centerline and 9 in. below the test bodies. The measured root-mean-square values are plotted as a function of cavitation number in Fig. 14. Since the free-air content of the river water was not measured, the extent of its influence on the noise measurement is not known. Barring this uncertainty, effect of body size is clearly demonstrated. For given nuclei, since the larger the body the longer the time allowed for a nucleus to expand before collapse, it is expected that  $R_0$  and maximum pressure are greater.

#### b. Wall Effect

In recent years considerable interest has been given to base-ventilated hydrofoils, reduction of drag force by ventilation, and similar effects. A completely air-cushioned hydrofoil is even being considered. The absorption or refraction of sound waves by a wall will complicate the noise problem. (A nonhemispherical bubble collapsing on a solid wall was theoretically treated by Naudé and Ellis [9]. They attributed cavitation damage to the high-speed jet which collides with the solid wall.)

A full-span wedge of 1 in. height and 13-degree vertex angle constructed for another purpose was used to test the effect of a solid wall on noise. The wedge was designed so that a 1/8-in. plate may be attached at its base dividing the wake into two symmetrical parts. Sound pressures due to cavitation were measured for cases with and without the dividing plate attached to the wedge. Figure 15(a) shows typical frequency spectra for the two cases at approximately equal  $\sigma$ . Except for a small shift in peak frequencies, the curves remained similar. For this particular  $\sigma$  the amplitude was much higher with the plate than without the plate. The root-mean-square values are plotted as functions of  $\sigma$  in Fig. 15(b). When the cavity is very small ( $\sigma > 0.8$ ), the effect of the wall is small. The effect of the wall is greatest when cavity noise is strongest (at moderate  $\sigma$ ), perhaps because of reflection and resonance of the wall.

#### B. High-Frequency Measurement

Resonant frequencies of bodies, as discussed earlier, occur mostly at low frequencies and the low-frequency measurements are not free from distortion. It was, therefore, considered necessary to take some measurements

covering the higher-frequency range. The frequency range covered under this part of the study is 1 kcps to 150 kcps. This is also the range where most work had been done by previous investigators [10, 11]. A piece of barium titanate crystal as described in section II was used as a pressure transducer. The transducer was calibrated against a standard hydrophone and its frequency response was determined and plotted in Fig. 16. The selectivity curve of the analyzer is shown in Fig. 5(b).

#### 1. Oscillographic Records of Background and Cavitation Noise

One of the difficulties in using a barium titanate crystal as a pressure transducer is its sensitivity to external noise. Although the crystal was insulated from the test body by means of rubber cement, the noise transmitted through the test body could not be completely sealed off. An oscillographic record of a noncavitating flow taken at a time when external noise is low is shown in Fig. 17(a). The response of the pressure transducer to noises coming from the nearby machine shop is shown in Fig. 17(b) and Fig. 17(c). All cavitation noise data were taken when these extreme external noises were absent. However, all external sources of noise and interference could not be completely eliminated.

When the external noise level is not too high, the oscillographic records thus obtained are very similar to the records obtained by the diaphragm transducer. Typical records are shown in Fig. 18. They show essentially the same trends as shown in Fig. 2.

It may be worthwhile to point out that the test body could be rotated so that the transducer could face any direction: upstream, downstream, or sideways. All the records shown in Figs. 16, 17, and 18 are for the transducer faced directly upstream. The noise levels indicated by the transducer at different positions were not necessarily identical. It was found that the noise level was higher at the rear end of the body than at the front when the cavity was short or transient. For a long cavity, on the other hand, the noise levels picked up by the crystal transducer at the two positions were about the same. This fact is illustrated in Fig. 19. As was stated before, it is believed that the pressure fluctuation inside a long steady cavity is much smaller than that outside of the cavity. The noise picked up by the crystal transducer facing downstream must, therefore, be transmitted through the test body from

the outside region. For the remaining part of the paper, it should be understood that noise was measured at the front end of the body.

## 2. Frequency Spectrum of Cavitation Noise

For the range of frequencies considered in this section, Mellen's [11] experiment is particularly interesting. He rotated a 1/16-in. rod in water with such a high speed as to create cavitation near the surface of the rod. The cavitation noise was measured at a distance of 1 meter from the rod. The frequency spectrum reported in [11] is reproduced in Fig. 20(a). A typical frequency spectrum obtained in the free-jet water tunnel for a 1/2-in. circular cylinder is shown in Fig. 20(b). Here the solid line is the part of the spectrum measured by means of the barium titanate crystal and the dotted line is a schematic drawing of the spectrum which would be measured by the diaphragm-type transducer. The present result resembles the result of Mellen for frequencies greater than 0.6 kcps. The only difference is that the present result has more peaks at lower frequencies.

It should be noted that the average slope for the frequency range from 5 kcps to about 80 kcps of the frequency spectrum shown in Fig. 20(b) and all the figures thereafter is about -6 db/octave. According to Benjamin [4], this indicates that the pressure wave is a pulse or a shock wave. The average slope of the frequency spectra for the higher frequency is about -12 db/octave and this may be attributable to the resonance of the transducer [4].

Frequency spectra of natural cavities for various  $\sigma_v$  are presented in Fig. 21 in three groups according to the range of  $\sigma_v$ : high, intermediate, and low. Figure 21 confirms the trend of the low-frequency measurements stated in section A. That is, the noise first increases, reaching a plateau, and then decreases as the reference cavitation number is being decreased from that of no cavitation to that of a long steady cavity.

Effect of ventilation on high-frequency noises is shown in Fig. 22. Part (a) of Fig. 22 indicates that ventilation actually increases the noise level if the original flow has very low noise level, i.e., if the original flow is noncavitating or at the beginning of transient cavitation. Part (b) of Fig. 22 shows that ventilation reduces all the frequency components of the noise if the original flow has high noise level. The last part of Fig. 22 is for relatively low  $\sigma_v$  where the original noise level is also low. In this case the effect of ventilation on the cavitation noise is small.

## IV. CONCLUSION

The present experiment was carried out in a free-jet tunnel which was not specifically designed for noise measurements. Protection against external noise was not provided. Vibration of the tunnel structure and the refraction of sound waves within the tunnel could not be eliminated. Consequently, some of the data are hard to interpret. Nevertheless, the following conclusions can safely be drawn:

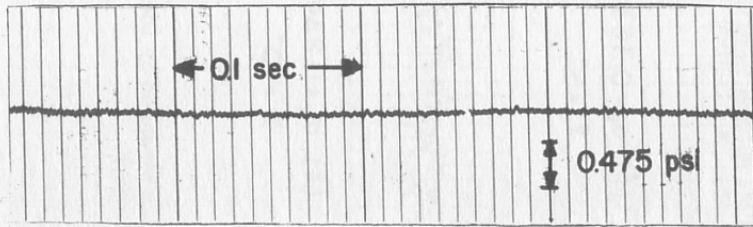
- (1) Noise level of natural cavities is a function of the reference cavitation number  $\sigma_v$ . As  $\sigma_v$  is decreased from the noncavitating condition, the noise increases at first as transient cavitation is established. Further decrease in  $\sigma_v$  finds the noise level reaching a plateau and then decreasing as the cavity becomes steady and increases in length.
- (2) Ventilation reduces cavitation noise over a wide range of cavitating conditions. However, if  $\sigma_v$  is very high so that little or no natural transient cavitation occurs, ventilation increases the noise by producing transient bubbles. On the other hand, for small  $\sigma_v$  where the cavity is long and steady, ventilation has little effect on cavity noise unless enough air is added to produce a pulsating cavity.
- (3) Cavitation noise also changes with size of the cavitating body. The larger the body, the larger is the cavitation noise.
- (4) Presence of a solid wall near the cavitating region tends to increase the cavitation noise.

L I S T O F R E F E R E N C E S

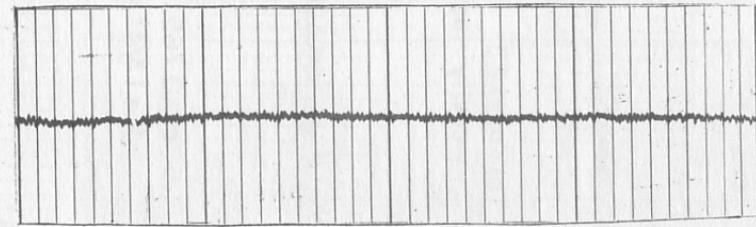
- [1] Eisenberg, P. "A Brief Survey of Progress on the Mechanics of Cavitation," David Taylor Model Basin Report No. 842. June 1953. 38 pages.
- [2] Silberman, E. and Song, C. S. "Instability of Ventilated Cavities," Journal of Ship Research, Vol. 5, No. 1, pp. 13-33. June 1961.
- [3] Song, C. S. Pulsation of Ventilated Cavities. University of Minnesota, St. Anthony Falls Hydraulic Laboratory Technical Paper No. 32-B. February 1961. 35 pages.
- [4] Benjamin, T. B. "Pressure Waves from Collapsing Cavities," Second Symposium on Naval Hydrodynamics, pp. 207-233. August 1958.
- [5] Silberman, E. and Ripken, J. F. The St. Anthony Falls Hydraulic Laboratory Gravity-Flow Free-Jet Water Tunnel. University of Minnesota, St. Anthony Falls Hydraulic Laboratory Technical Paper No. 24-B, April 1959. 45 pages.
- [6] Hueter, T. F. and Bolt, R. H. Sonics. John Wiley and Sons, Incorporated, p. 235, Fig. 6-16. 1955.
- [7] Harrison, M. "An Experimental Study of Single Bubble Cavitation Noise," David Taylor Model Basin Report No. 815. November 1952. 20 pages.
- [8] Kermeen, R. W. "Some Observations of Cavitation on Hemispherical Head Models," California Institute of Technology Engineering Division Report No. 35-1. June 1952. 30 pages.
- [9] Naudé, C. F. and Ellis, A. T. "On the Mechanism of Cavitation Damage by Non-Hemispherical Cavities Collapsing in Contact with a Solid Boundary," California Institute of Technology Engineering Division Report No. 108-7. July 1960. 21 pages.
- [10] Fitzpatrick, H. M. and Strasberg, M. "Hydrodynamic Sources of Sound," David Taylor Model Basin Report No. 1269. January 1959. 41 pages.
- [11] Mellen, R. H. "Ultrasonic Spectrum of Cavitation Noise in Water," Journal Acoustic Society of America, Vol. 26, p. 356. 1954.



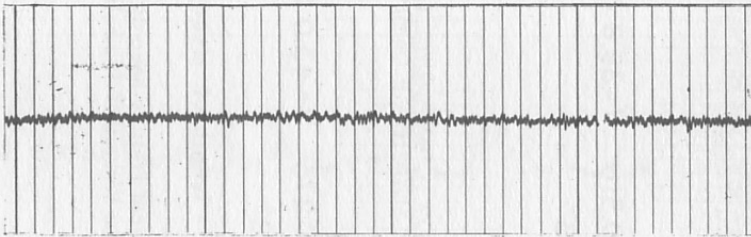
F I G U R E S  
(1 through 22)



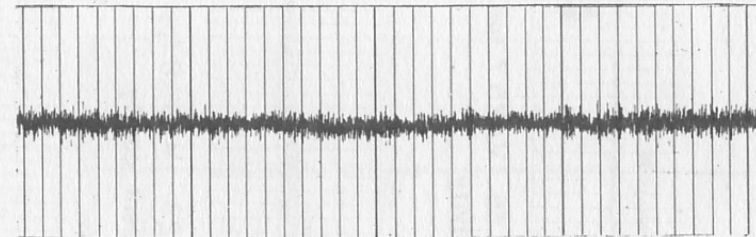
(a)  $\sigma_v = 2.59$        $V = 25.6$  fps



(b)  $\sigma_v = 1.16$        $V = 34.6$  fps

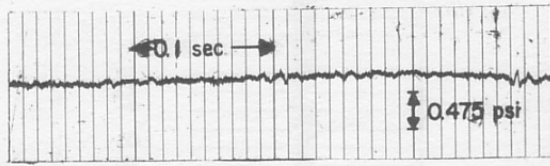


(c)  $\sigma_v = 0.445$        $V = 40.6$  fps

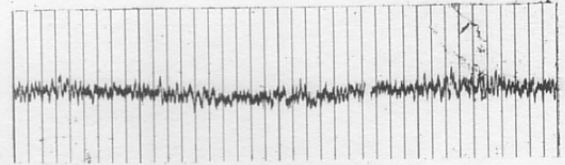


(d)  $\sigma_v = 0.131$        $V = 44.9$  fps

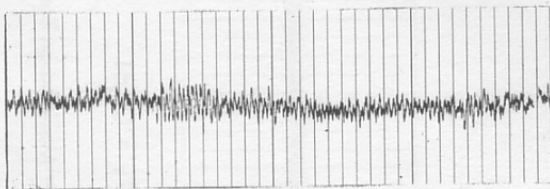
Fig. 1 - Background Noise Picked Up by Diaphragm-Type Transducer Mounted on Tunnel Wall



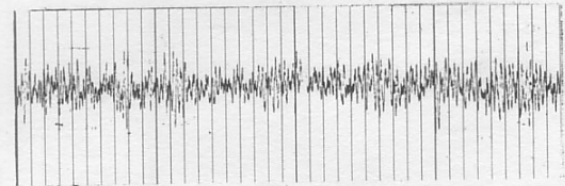
(a)  $\sigma_v = 2.35$   $V = 25.7$  fps  
no cavity



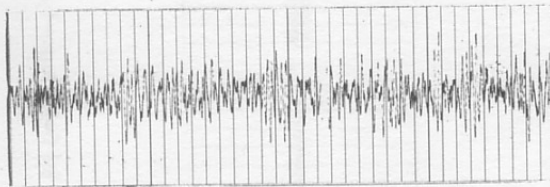
(b)  $\sigma_v = 1.23$   $V = 32.7$  fps  
cavity just started



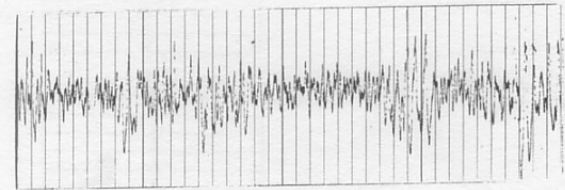
(c)  $\sigma_v = 1.23$   $V = 33.8$  fps  
transient cavity



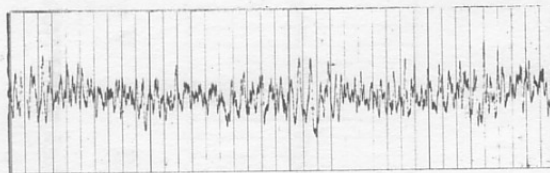
(d)  $\sigma_v = 0.765$   $V = 37.5$  fps  
 $l = 1\frac{3}{4}$ "



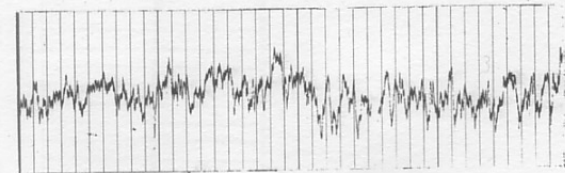
(e)  $\sigma_v = 0.510$   $V = 39.8$  fps  
 $l = 3$ "



(f)  $\sigma_v = 0.363$   $V = 41.5$  fps  
 $l = 5$ "



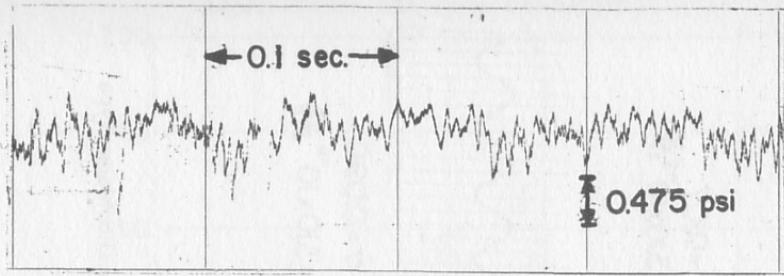
(g)  $\sigma_v = 0.275$   $V = 43.0$  fps  
 $l = 8$ "



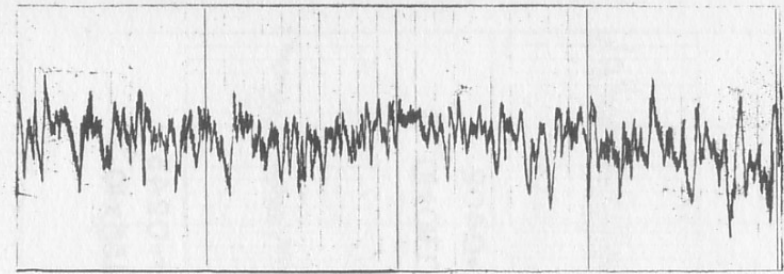
(h)  $\sigma_v = 0.234$   $V = 43.5$  fps  
 $l = 10$ "

NOTE:  $l$  = length of steady cavity

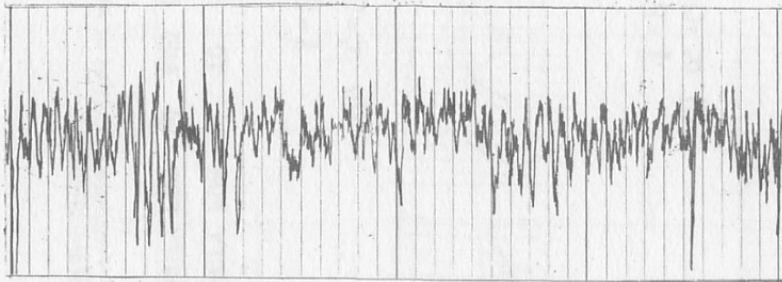
Fig. 2 - Typical Pressure Records of Natural Cavities as Measured by Diaphragm-Type Transducer Outside of the Wake (1/2-in. Full-Span Circular Cylinder)



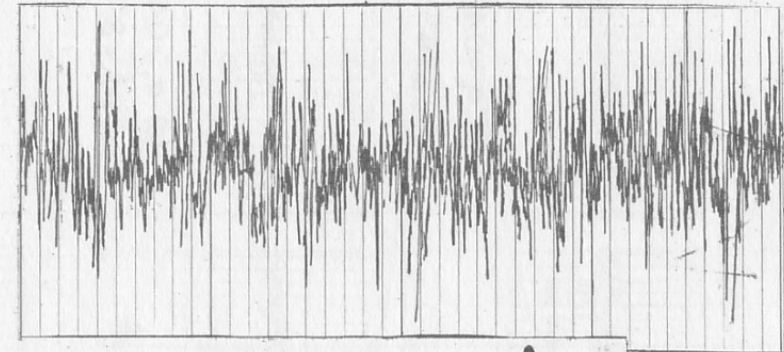
(a)  $\sigma_v = 2.56$   $V = 25.4$  fps. no cavity



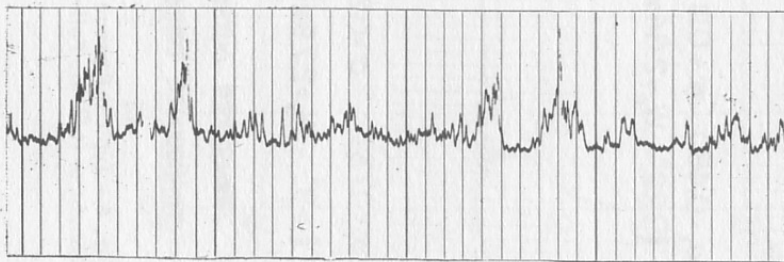
(b)  $\sigma_v = 1.87$   $V = 28.7$  fps. cavity just started



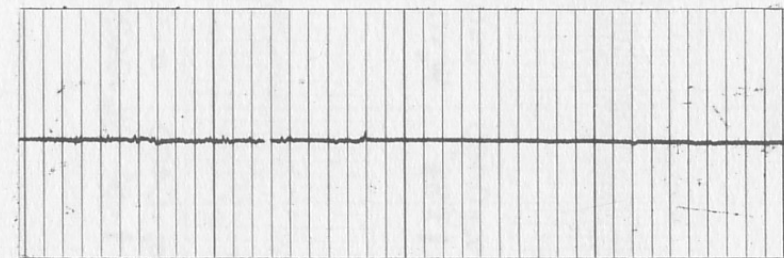
(c)  $\sigma_v = 1.13$   $V = 34.2$  fps. transient cavity



(d)  $\sigma_v = 0.579$   $V = 39.5$  fps.  $\lambda = 2''$

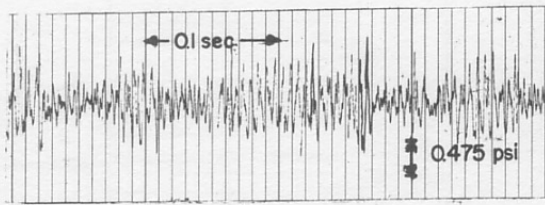


(e)  $\sigma_v = 0.252$   $V = 42.9$  fps.  $\lambda = 8''$

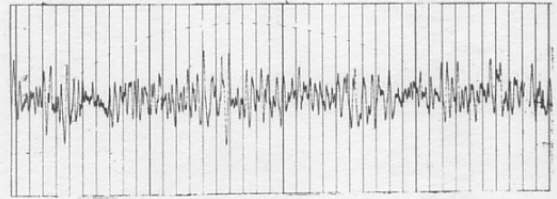


(f)  $\sigma_v = 0.199$   $V = 45.0$  fps.  $\lambda = 20''$

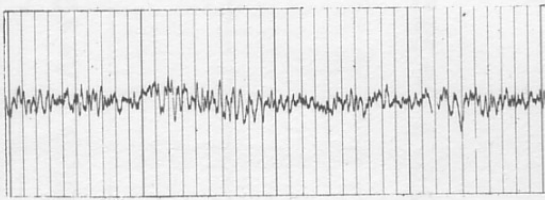
Fig. 3 - Typical Pressure Records of Natural Cavities as Measured by Diaphragm-Type Transducer in the Wake (1/2-in. Full-Span Circular Cylinder)



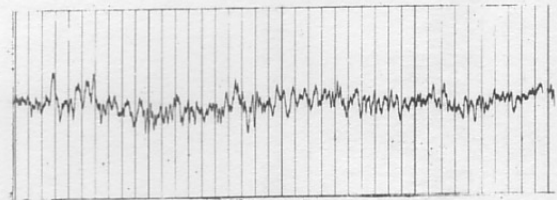
(a)  $\sigma_v = 0.460$      $\sigma = 0.443$   
 $\lambda = 3\frac{1}{2}''$      $W_a = 0 \frac{\text{lb}}{\text{sec}}$



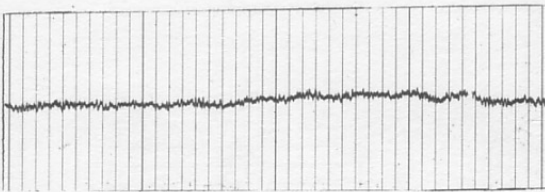
(b)  $\sigma_v = 0.460$      $\sigma = 0.402$   
 $\lambda = 4''$      $W_a = 0.310 \times 10^{-3} \frac{\text{lb}}{\text{sec}}$



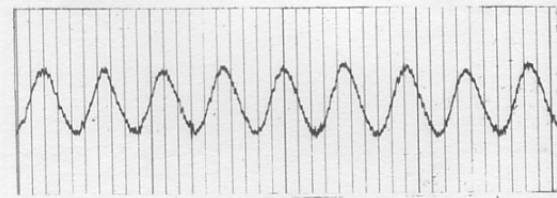
(c)  $\sigma_v = 0.460$      $\sigma = 0.345$   
 $\lambda = 5''$      $W_a = 0.620 \times 10^{-3} \frac{\text{lb}}{\text{sec}}$



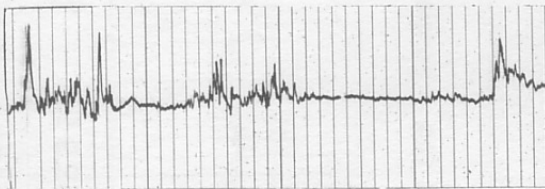
(d)  $\sigma_v = 0.460$      $\sigma = 0.243$   
 $\lambda = 8''$      $W_a = 1.55 \times 10^{-3} \frac{\text{lb}}{\text{sec}}$



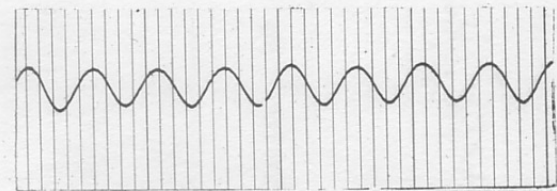
(e)  $\sigma_v = 0.460$      $\sigma = 0.111$   
 $\lambda = 22''$      $W_a = 2.64 \times 10^{-3} \frac{\text{lb}}{\text{sec}}$



(f)  $\sigma_v = 0.460$      $\sigma = 0.107$   
 $\lambda = 24''$      $W_a = 3.10 \times 10^{-3} \frac{\text{lb}}{\text{sec}}$



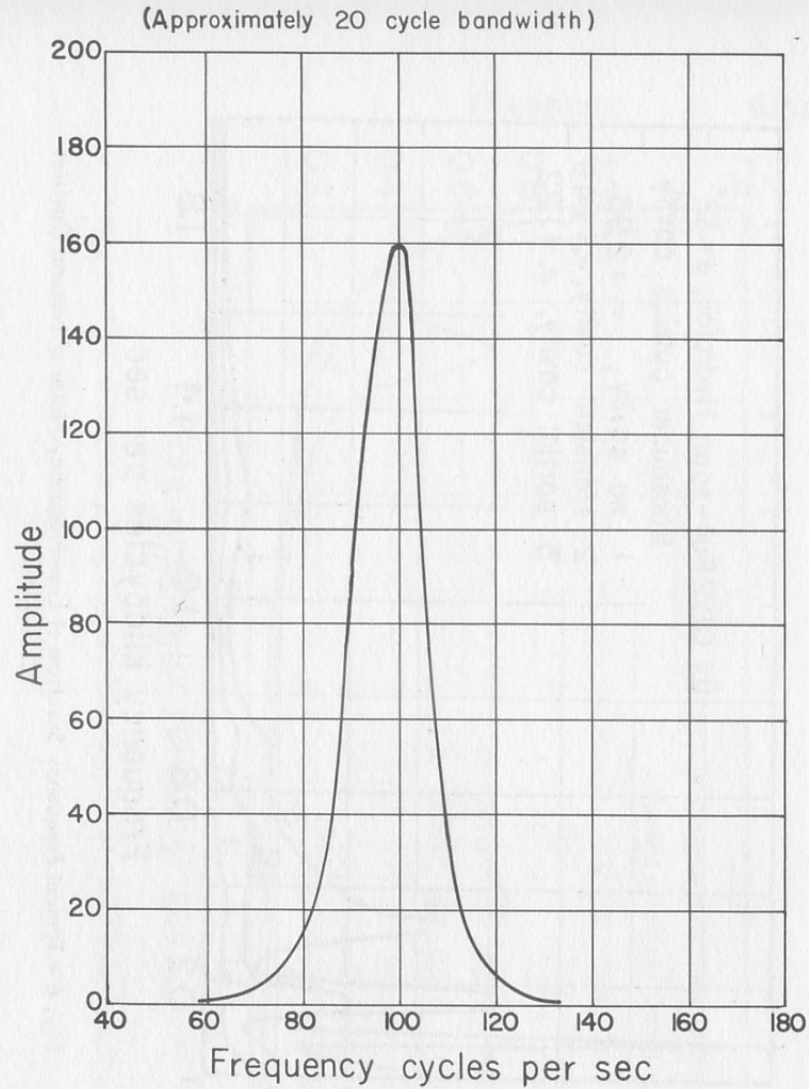
(g)  $\sigma_v = 0.737$      $\sigma = 0.226$   
 $\lambda = 9''$      $W_a = 2.79 \times 10^{-3} \frac{\text{lb}}{\text{sec}}$



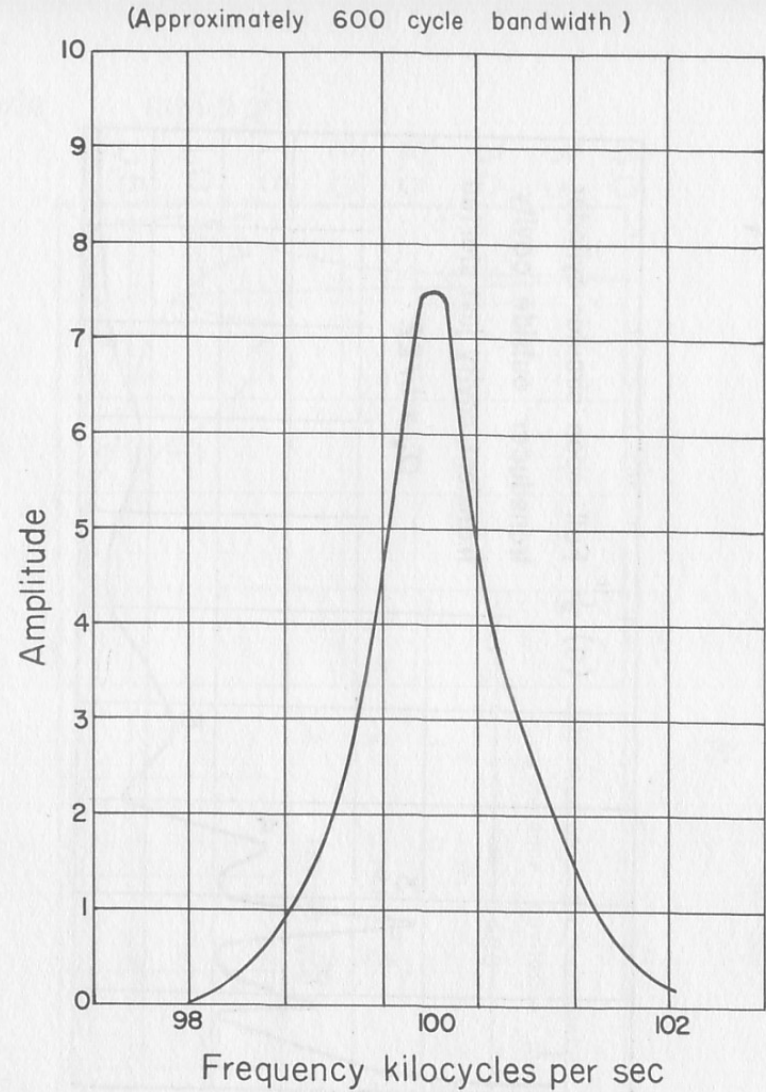
(h)  $\sigma_v = 0.430$      $\sigma = 0.090$   
 $\lambda = 24''$      $W_a = 3.10 \times 10^{-3} \frac{\text{lb}}{\text{sec}}$

NOTE: TRANSDUCER OUTSIDE OF CAVITY FOR (a) TO (f)  
 TRANSDUCER INSIDE OF CAVITY FOR (g) AND (h)

Fig. 4 - Typical Pressure Records of Ventilated Cavities as Measured by Diaphragm-Type Transducer (1/2-in. Full-Span Circular Cylinder)



a. Hewlett Packard 300A Harmonic Wave Analyzer



b. Panoramic Ultrasonic Analyzer

Fig. 5 - Response Characteristics of Hewlett Packard 300A Harmonic Wave Analyzer and Panoramic Ultrasonic Analyzer

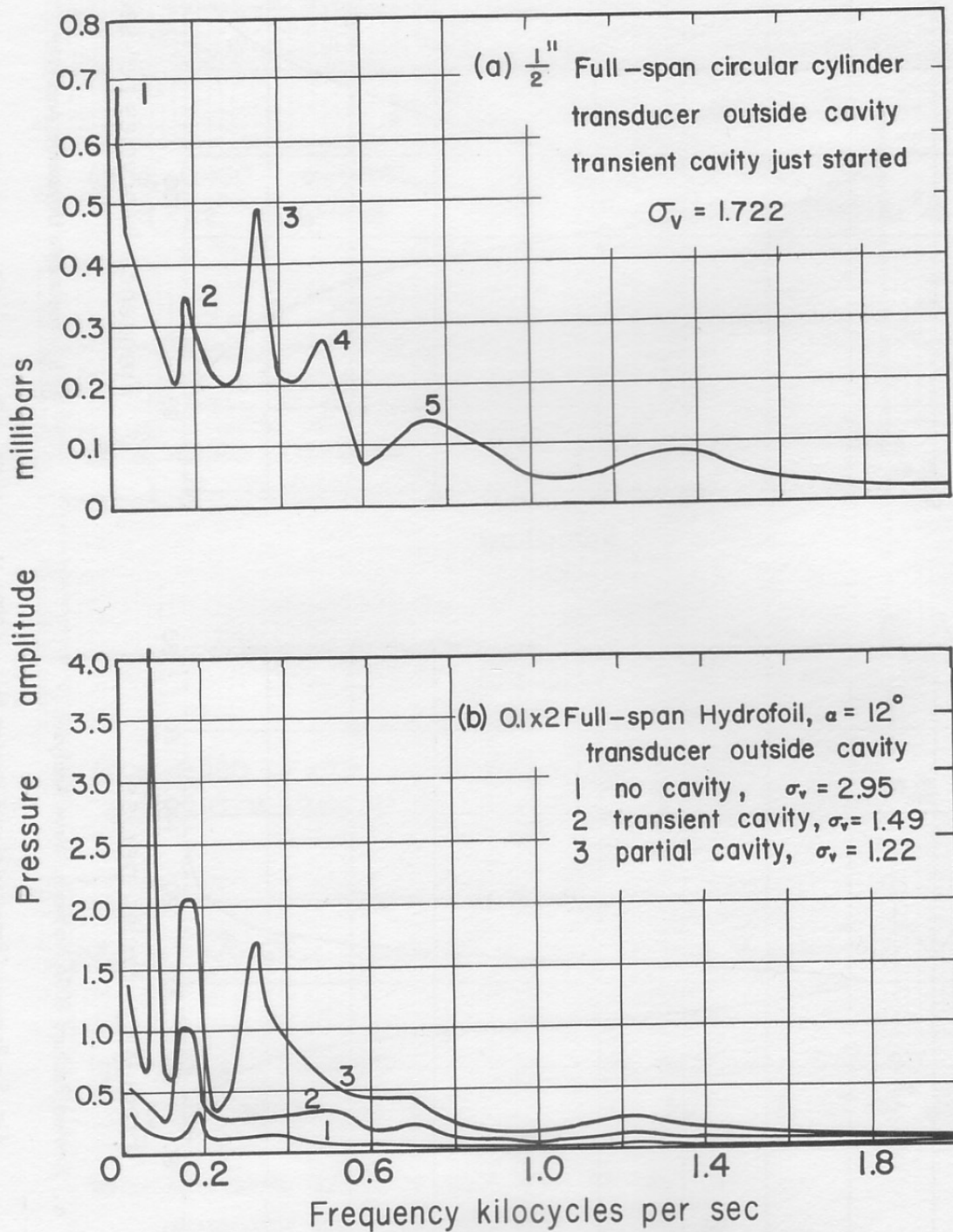


Fig. 6 - Typical Frequency Spectrum of Low-Frequency Noise of Natural Cavities

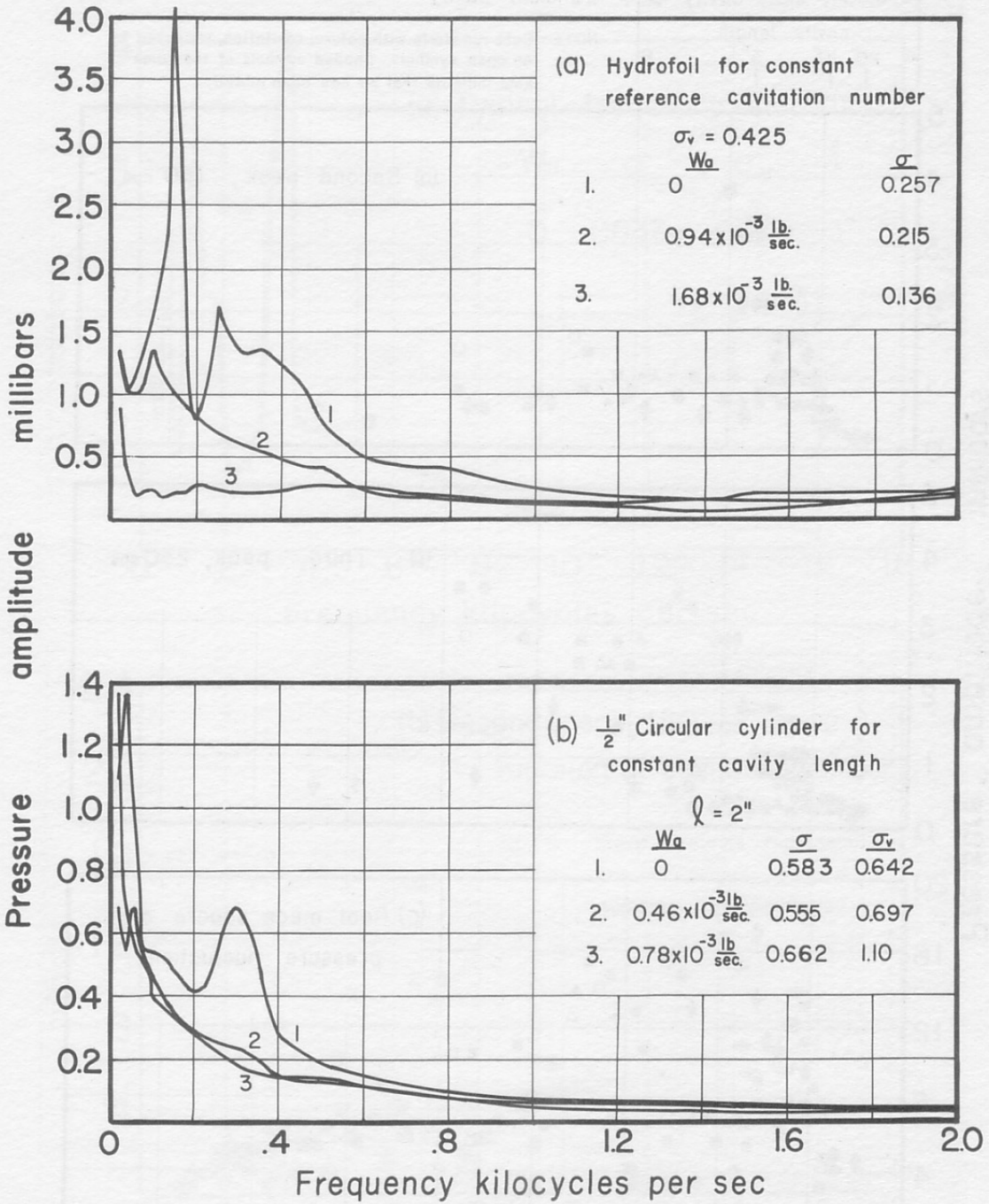


Fig. 7 - Typical Frequency Spectrum of Low-Frequency Noise of Ventilated Cavities



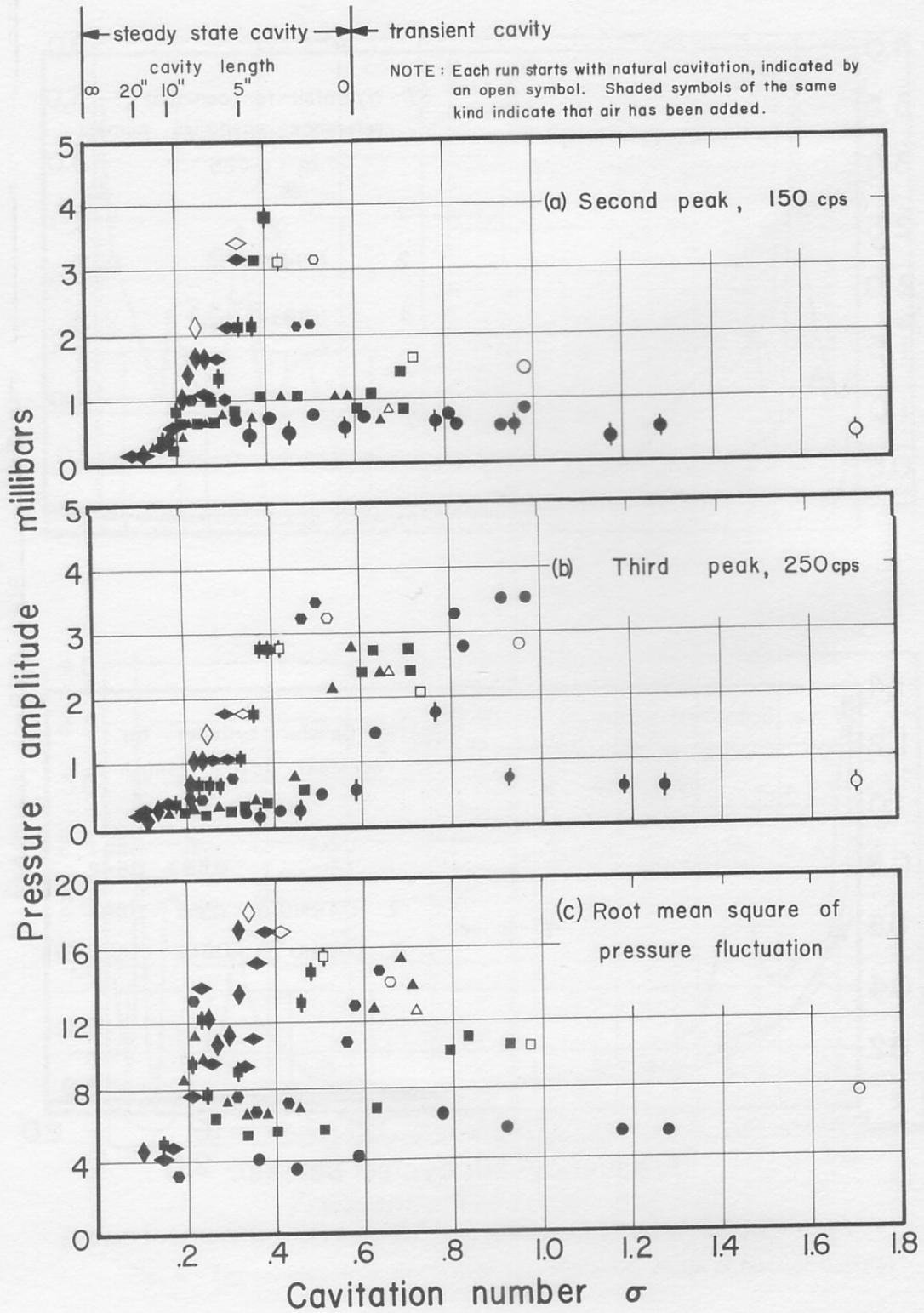


Fig. 8 - Pressure Amplitude as a Function of Cavitation Number (1/2-in. Full-Span Circular Cylinder)

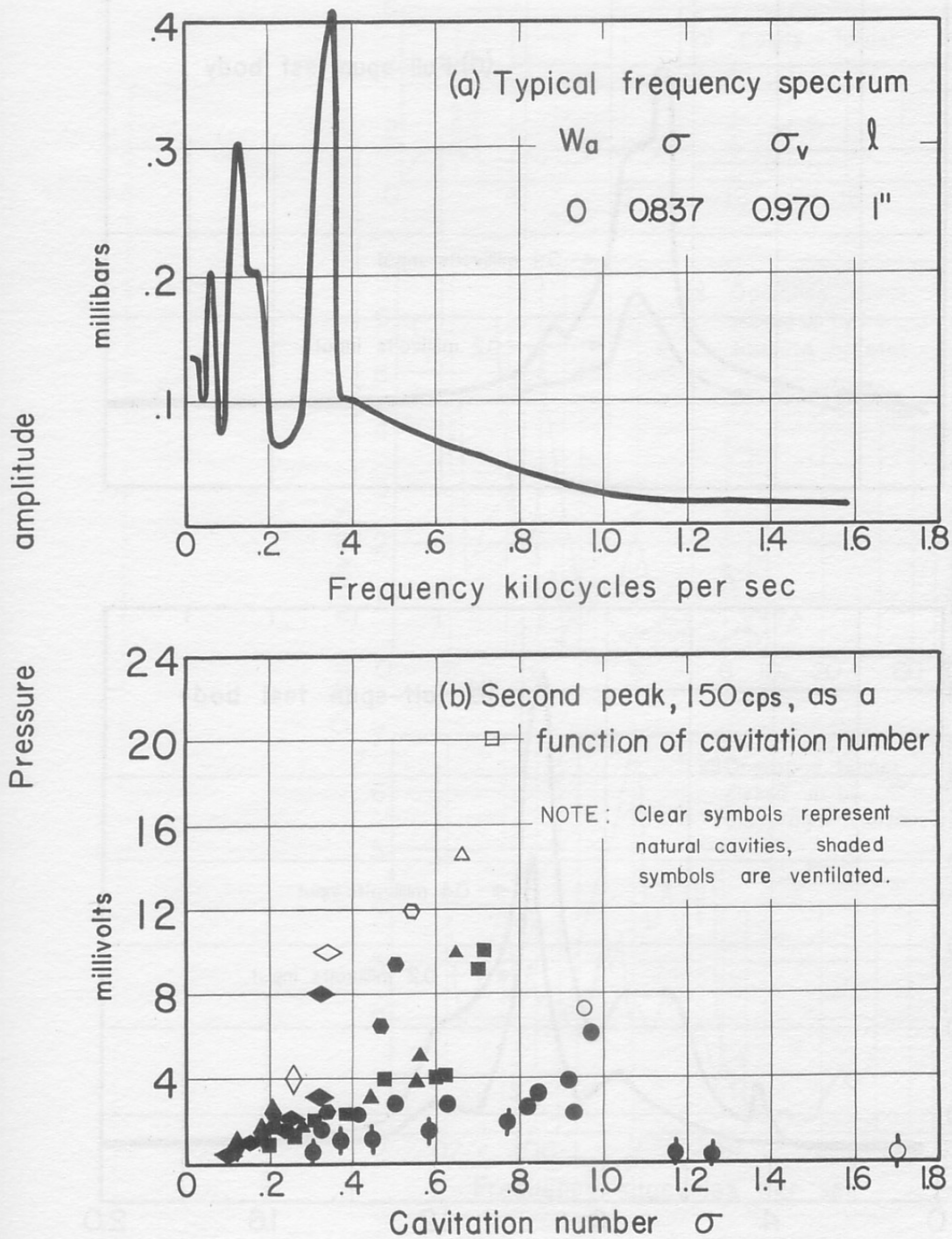


Fig. 9 - Low-Frequency Measurement Using a Barium Titanate Crystal as a Pressure Transducer (1/2-in. Full-Span Circular Cylinder)

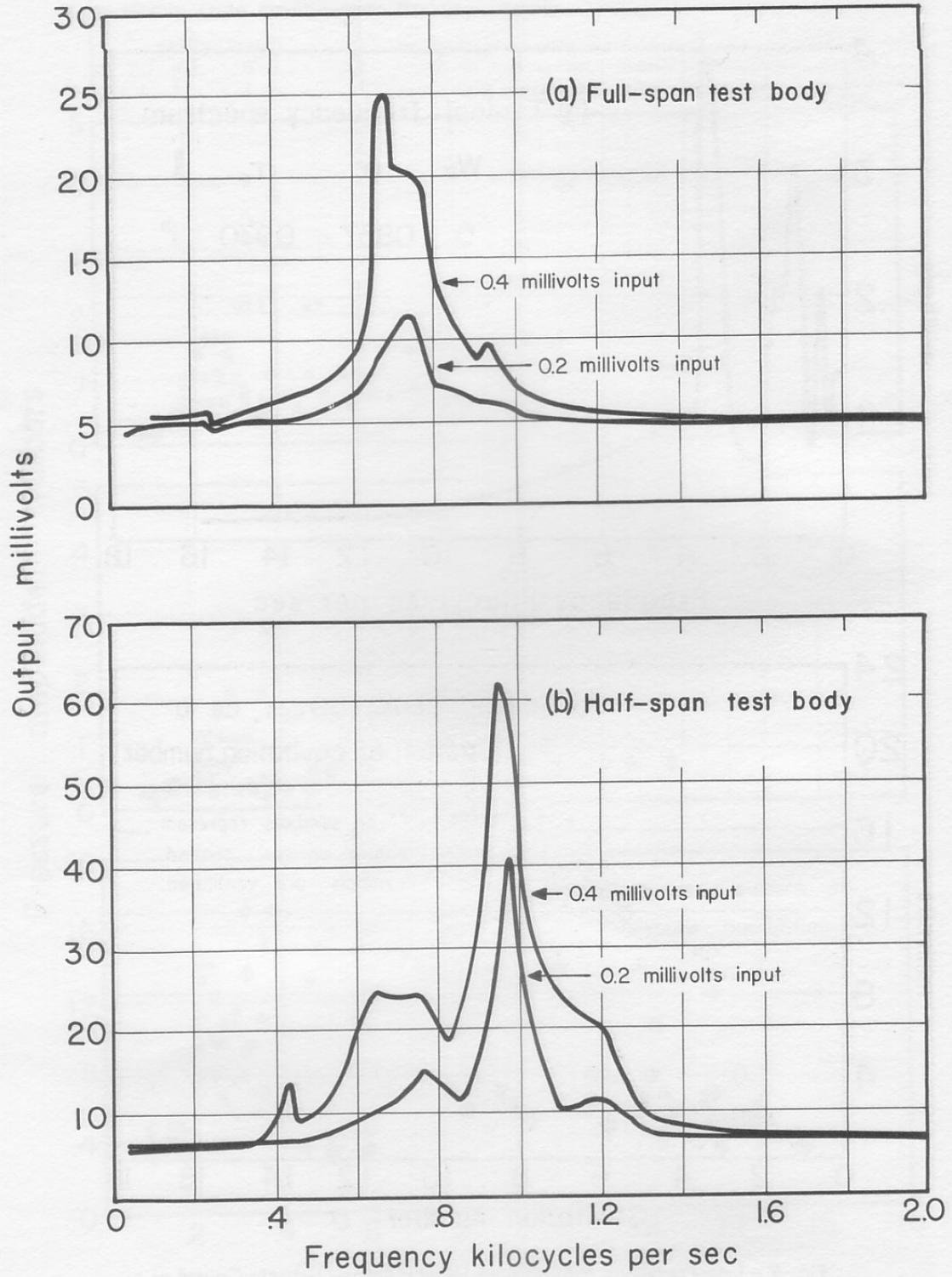


Fig. 10 - Resonance Frequency of 1/2-in. Circular Cylinders

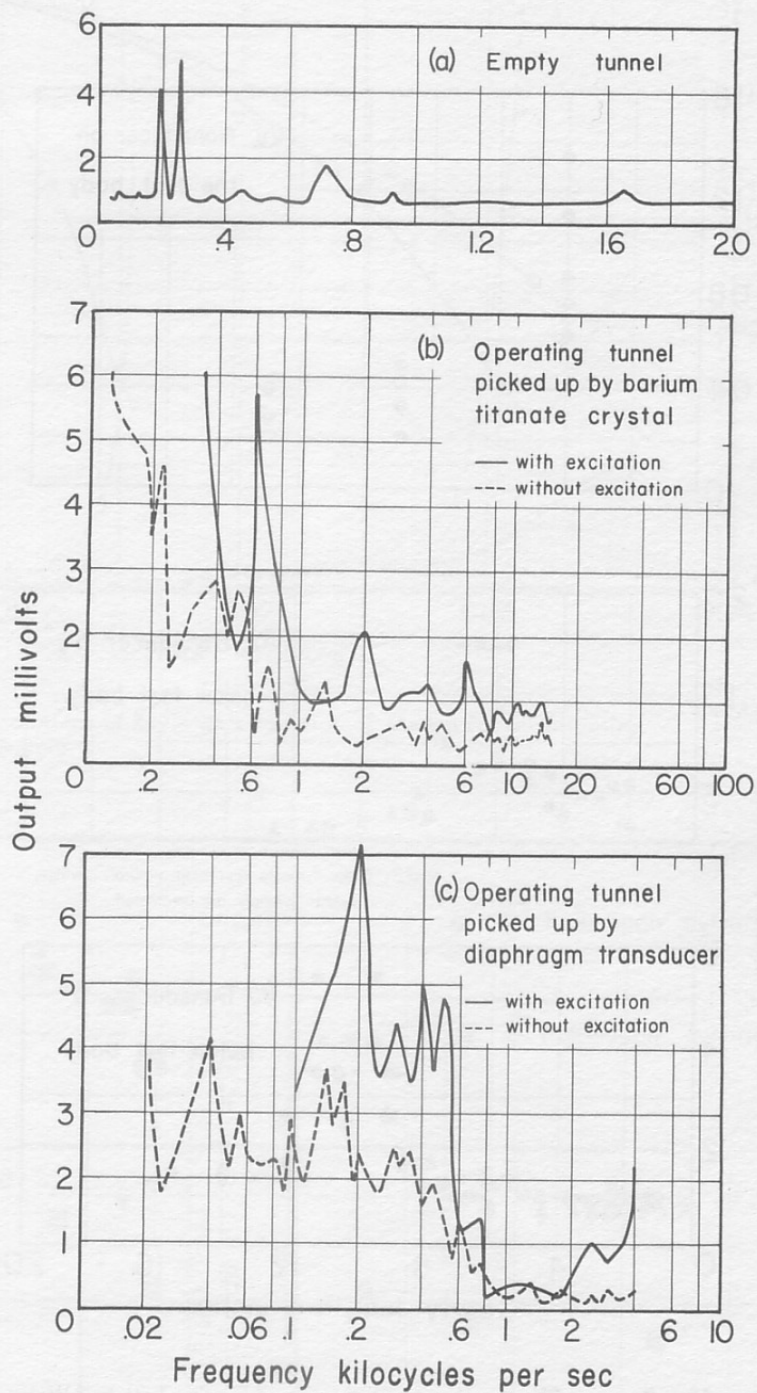


Fig. 11 - Resonance Frequencies of the Water Tunnel and Accessories

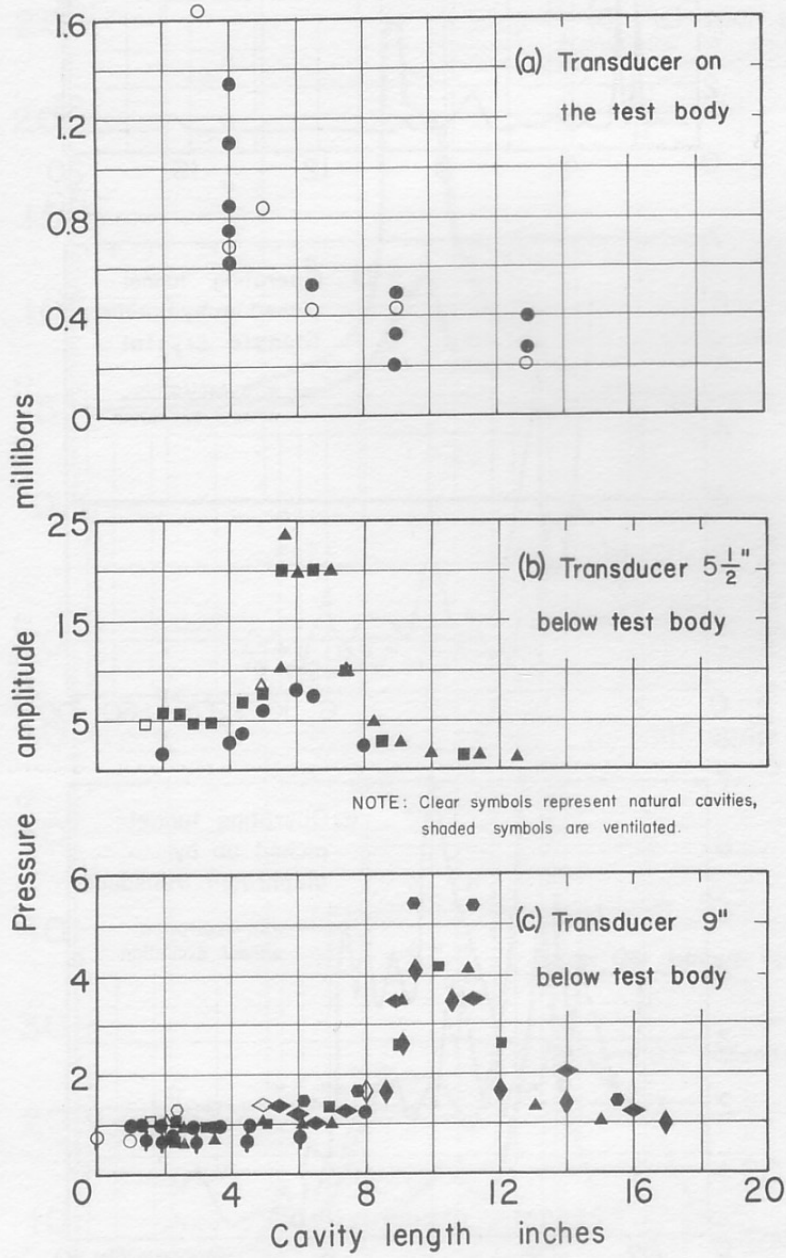


Fig. 12 - Pressure Change Due to Fluttering of Cavity Tail and Wake

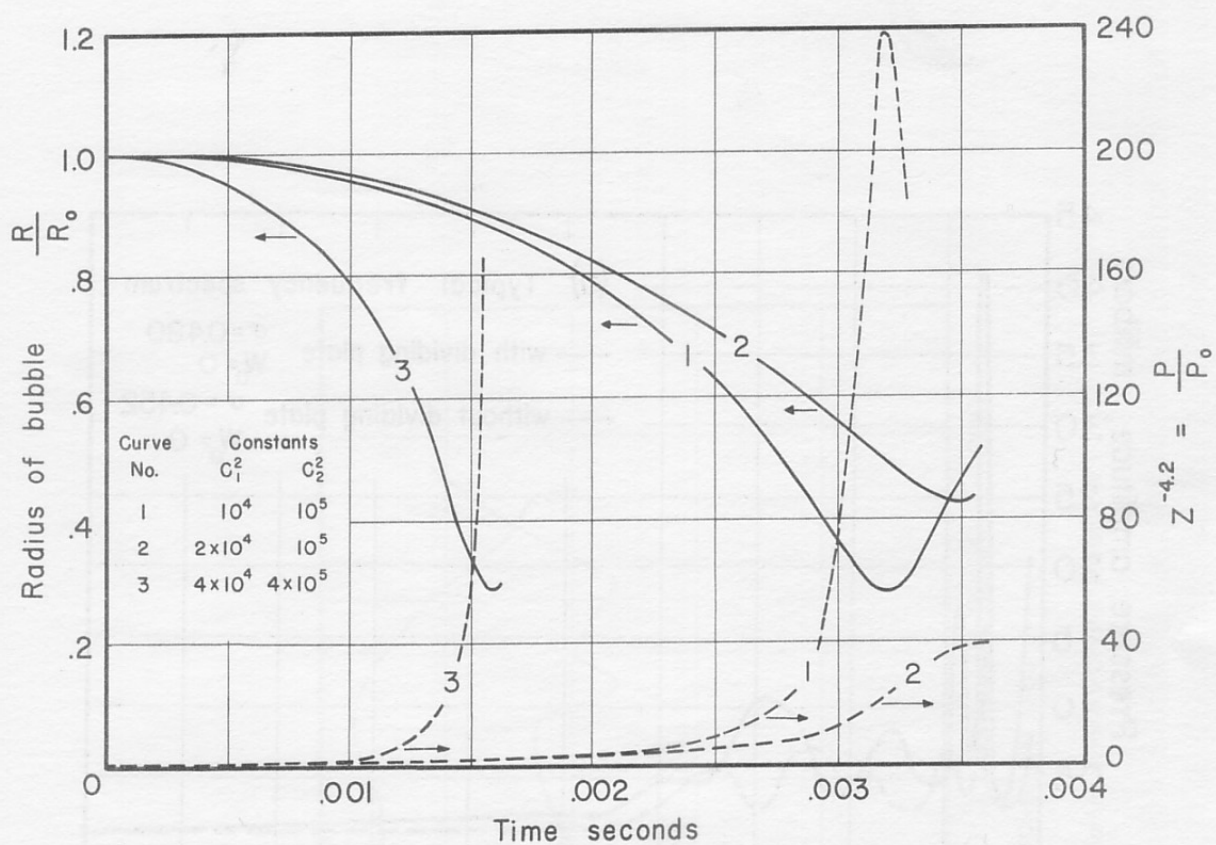


Fig. 13 - Solutions of Rayleigh's Equation of Motion for a Collapsing Spherical Bubble

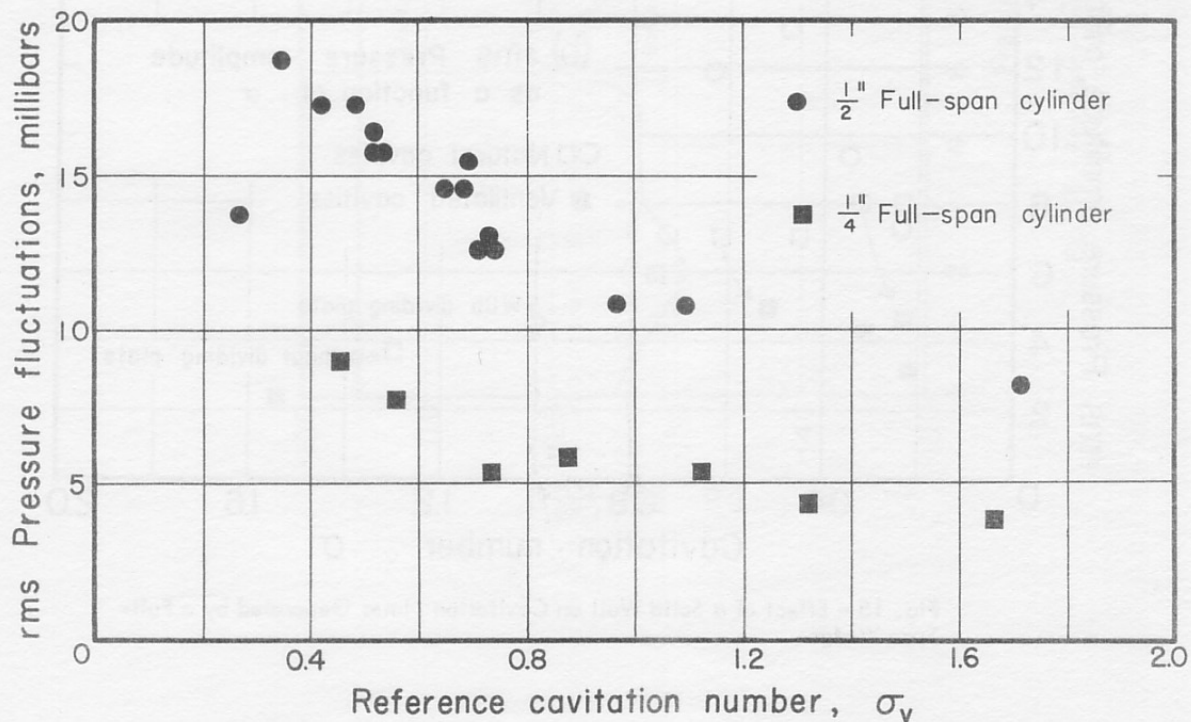


Fig. 14 - Effect of Body Size on Cavitation Noise

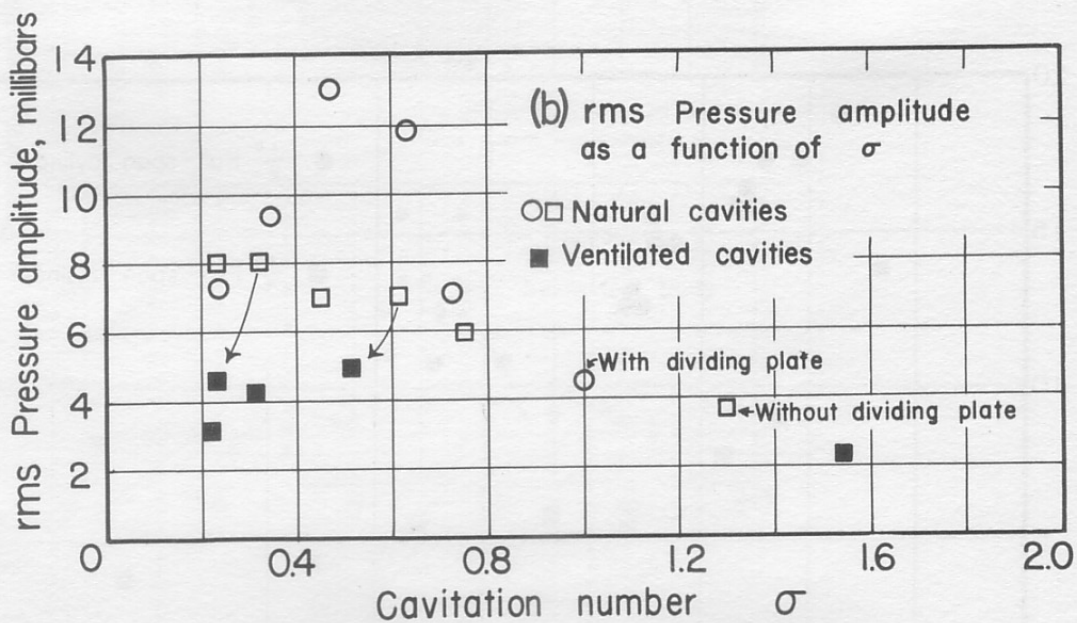
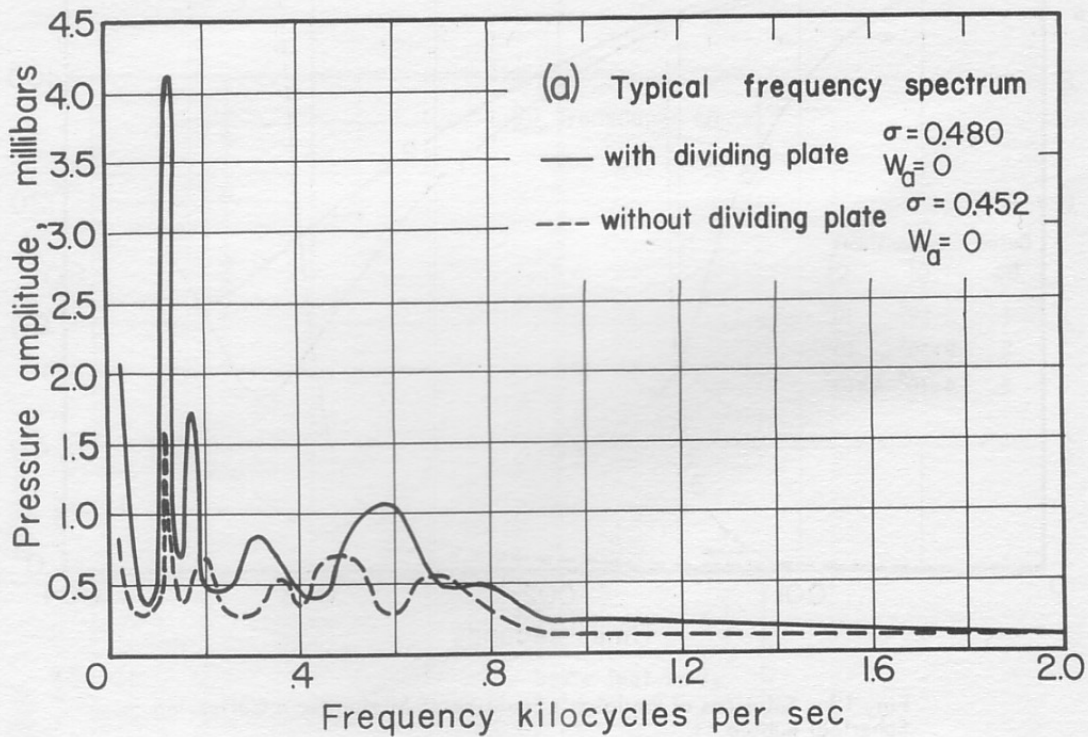


Fig. 15 - Effect of a Solid Wall on Cavitation Noise Generated by a Full-Span Wedge

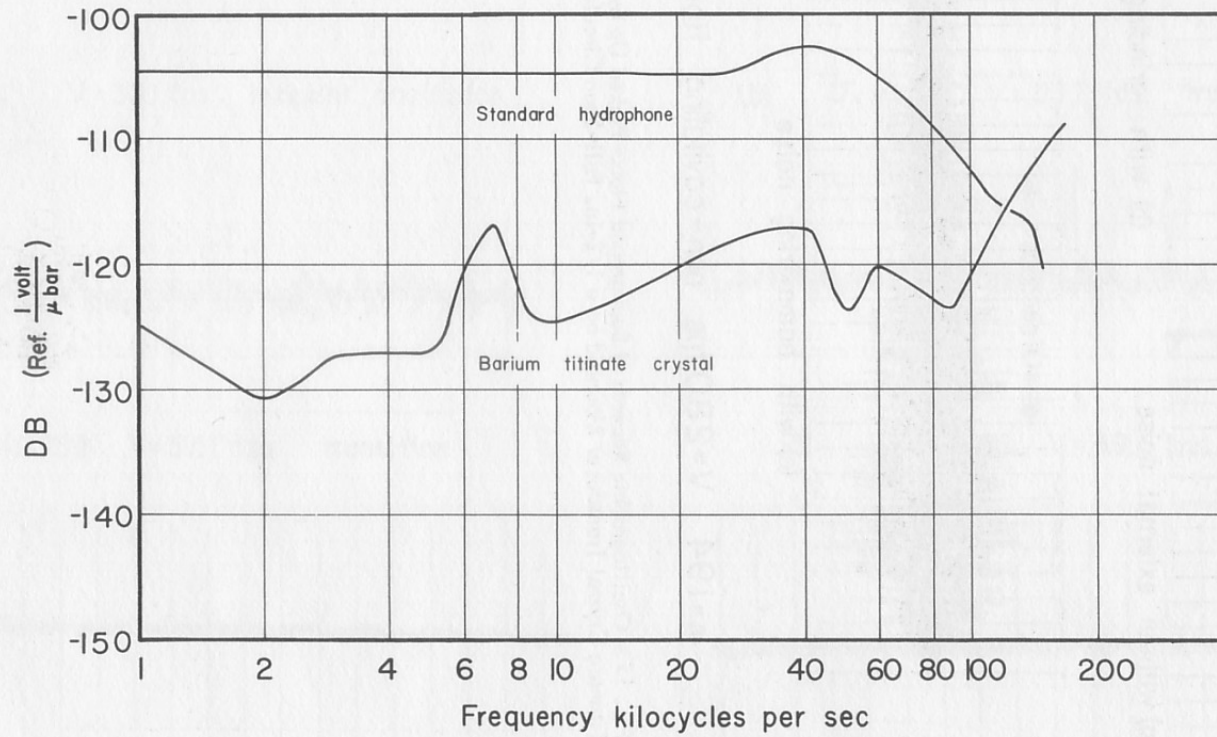
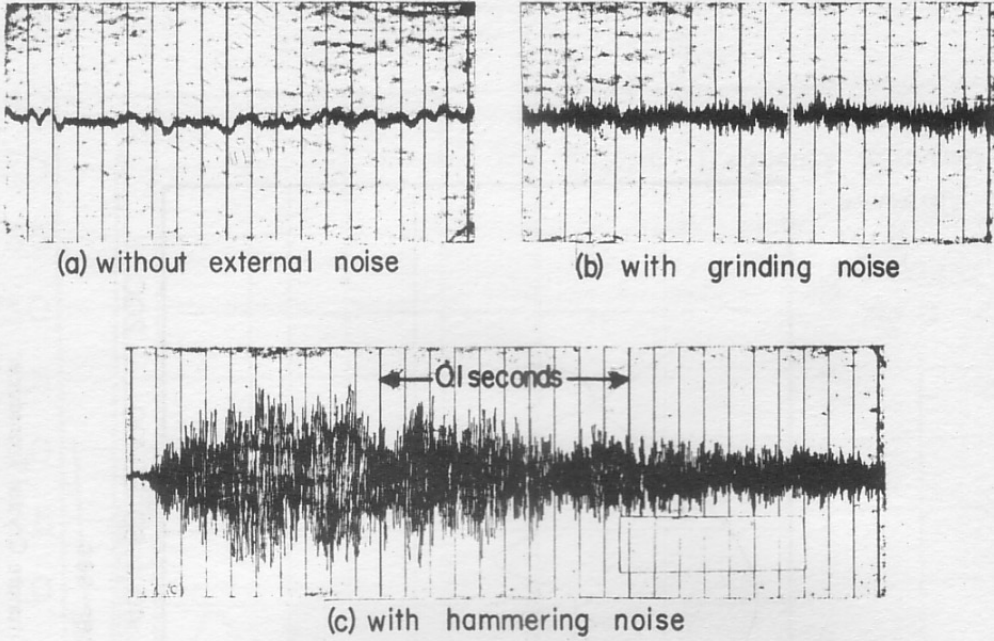


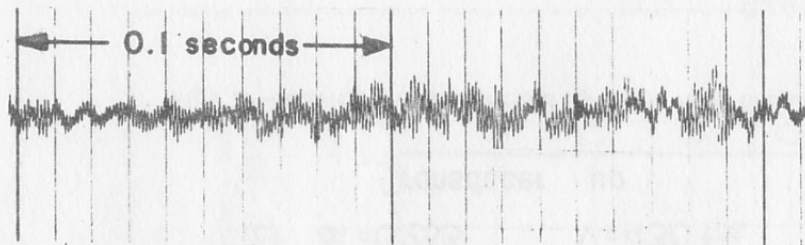
Fig. 16 - Frequency Response of the Barium Titanate Crystal Transducer



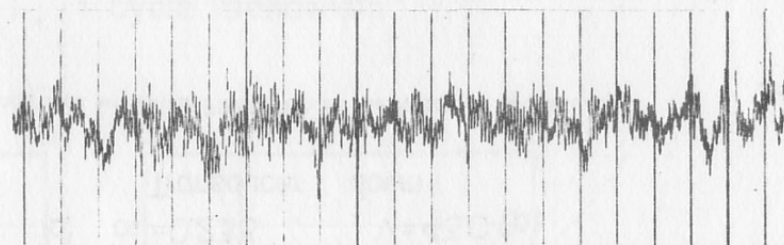


$\sigma_v = 1.94$   $V = 28.0$  fps. non-cavitating flow

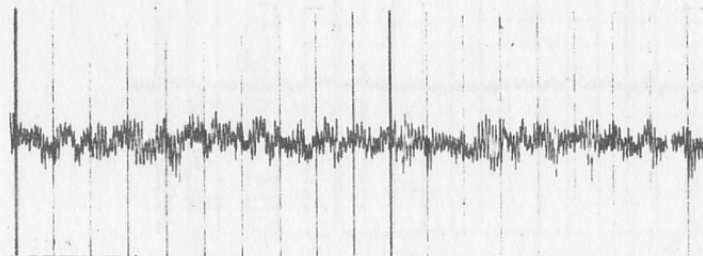
Fig. 17 - Oscillographic Records of Background Noise Picked Up by the Barium Titanate Crystal Transducer Mounted on a 1/2-in. Full-Span Circular Cylinder



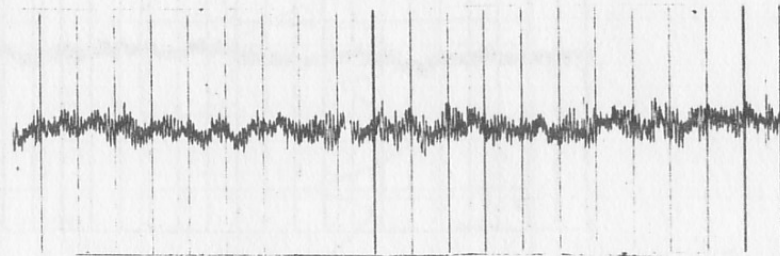
(a)  $\sigma_v = 1.51$   $V = 30.1$  fps incipient cavitation



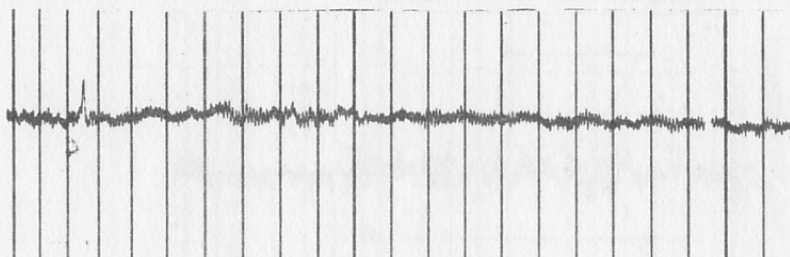
(b)  $\sigma_v = 1.00$   $V = 35.7$  fps transient cavitation



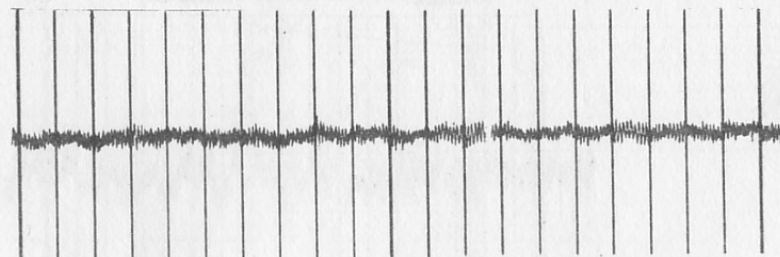
(c)  $\sigma_v = 0.759$   $V = 37.7$  fps transition



(d)  $\sigma_v = 0.549$   $V = 39.6$  fps  $\lambda = 2''$



(e)  $\sigma_v = 0.233$   $V = 43.0$  fps  $\lambda = 6''$



(f)  $\sigma_v = 0.125$   $V = 44.5$  fps.  $\lambda = 12''$

Fig. 18 - Typical Oscillographic Records of Cavitation Noise Picked Up by the Barium Titanate Crystal Transducer

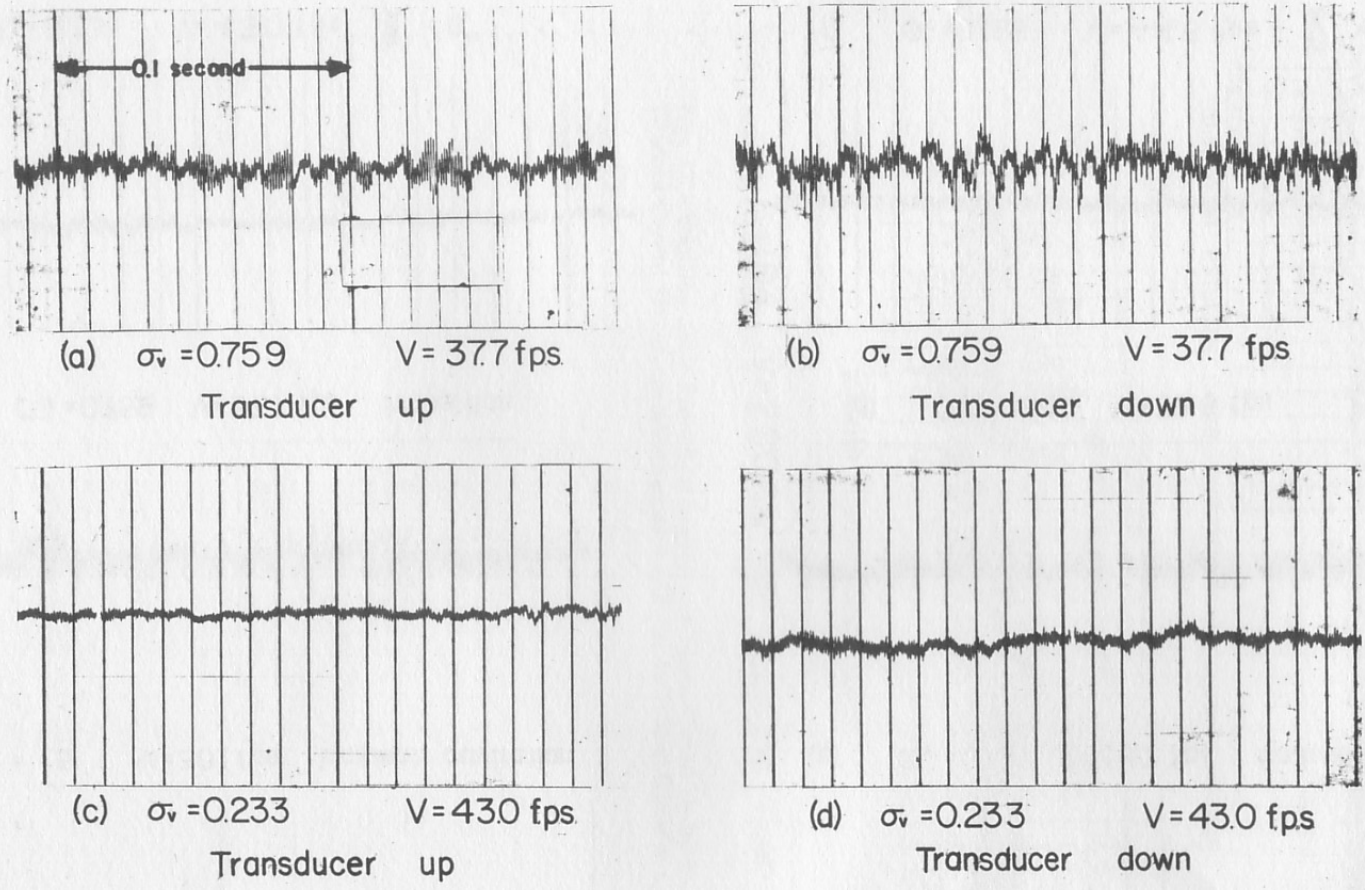


Fig. 19 - Cavitation Noise Picked Up at the Front End of the Body Compared with that Picked Up at the Rear End of the Body

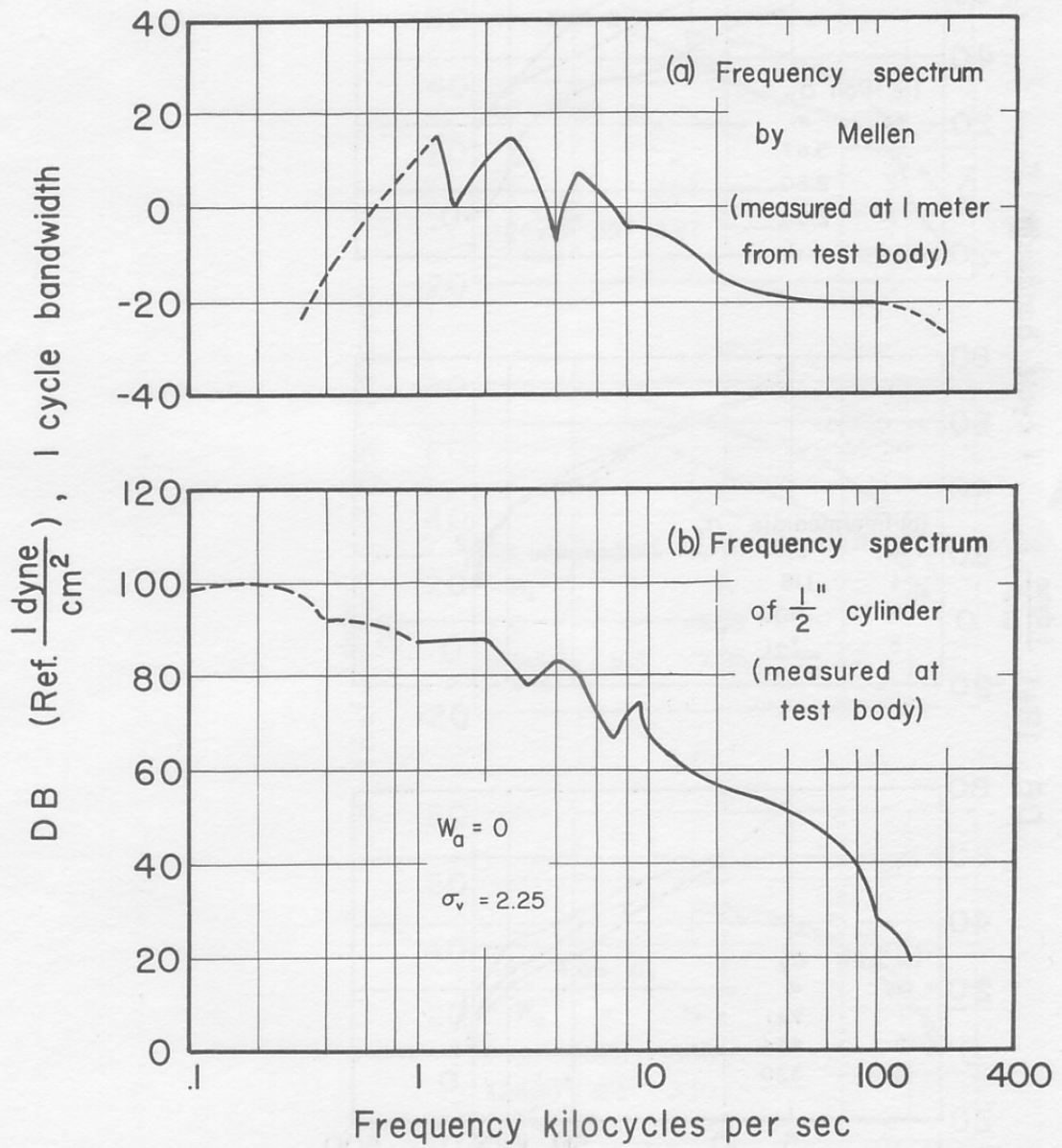


Fig. 20 - Typical Frequency Spectrum of Cavitation Noise at the Free-Jet Water Tunnel Compared with the Result of Mellen

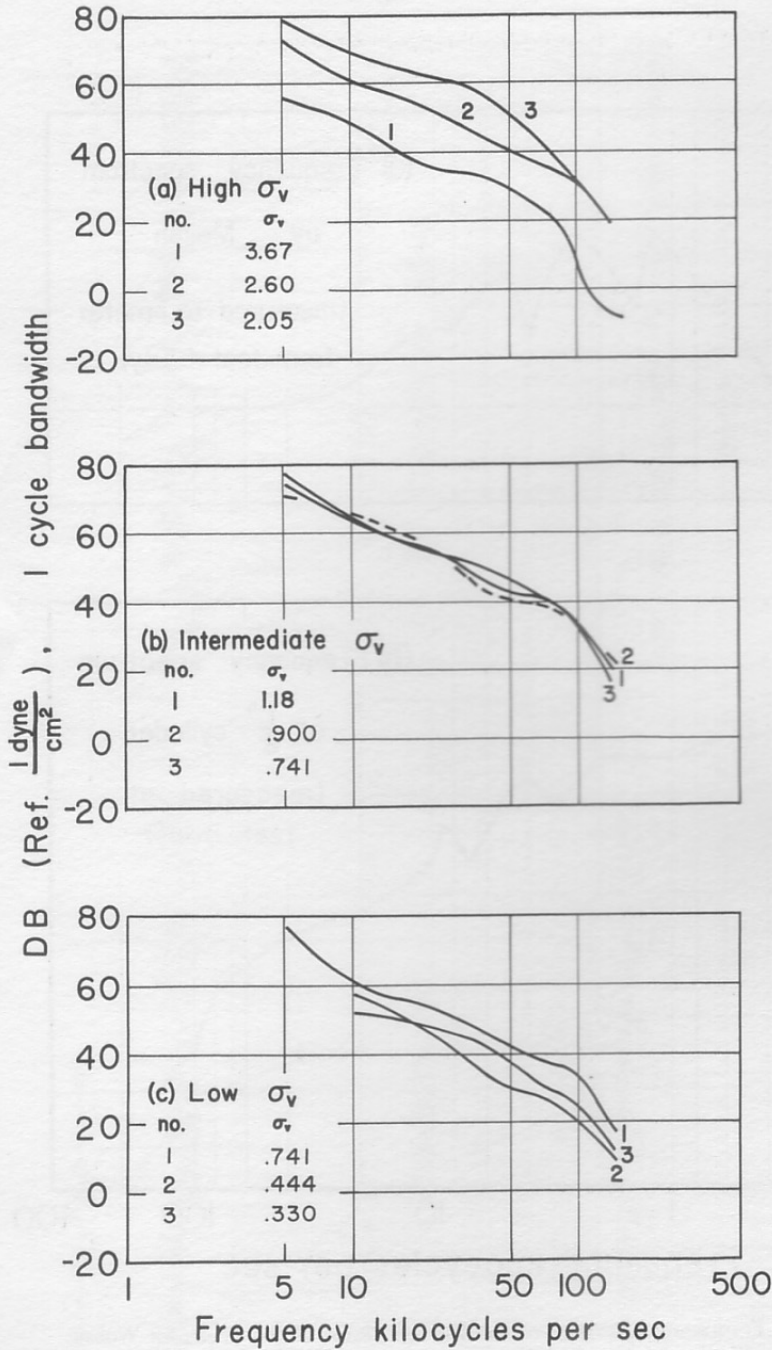


Fig. 21 - Frequency Spectra of Natural Cavities

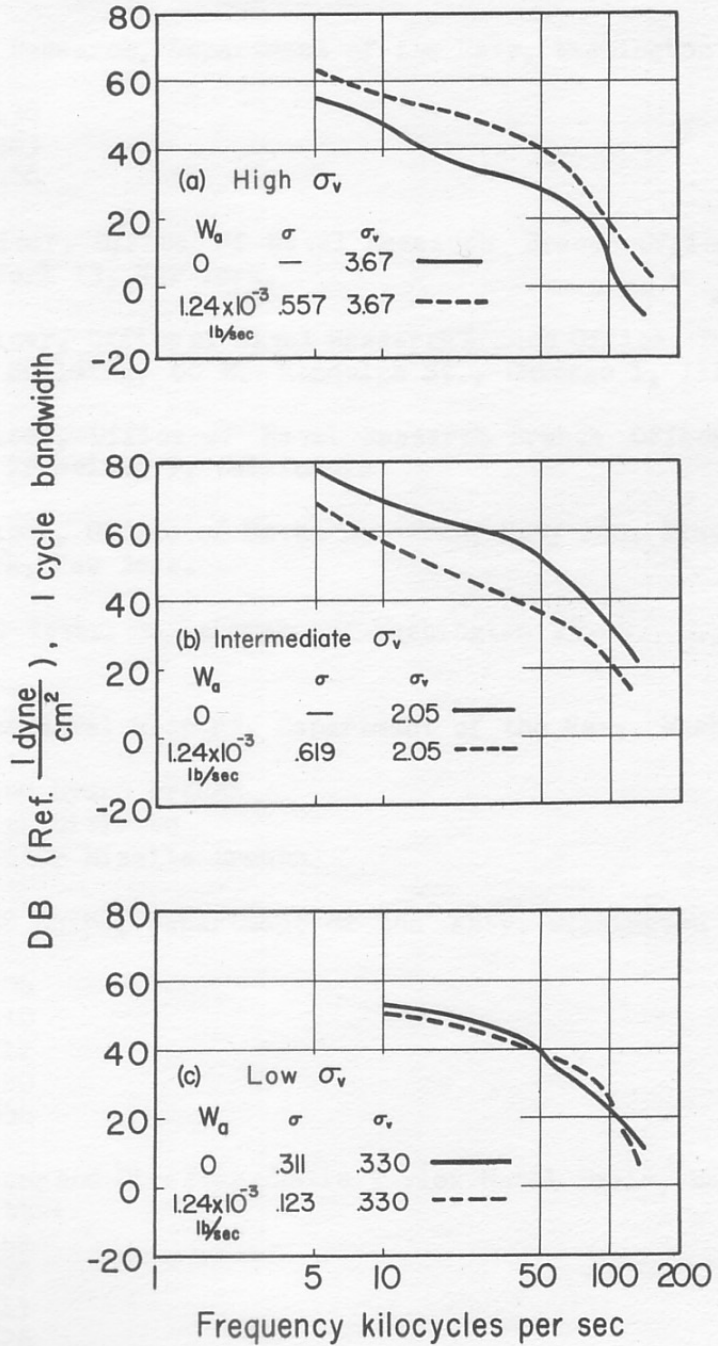


Fig. 22 - Frequency Spectra of Ventilated Cavities

SPONSOR'S DISTRIBUTION LIST FOR TECHNICAL PAPER NO. 33-B  
of the St. Anthony Falls Hydraulic Laboratory

<u>Copies</u>	<u>Organization</u>
5	Chief of Naval Research, Department of the Navy, Washington 25, D. C., Attn: 3 - Code 438 1 - Code 463 1 - Code 466
1	Commanding Officer, Office of Naval Research Branch Office, 346 Broadway, New York 13, New York.
1	Commanding Officer, Office of Naval Research Branch Office, The John Crerar Library Building, 86 E. Randolph St., Chicago 1, Illinois.
1	Commanding Officer, Office of Naval Research Branch Office, 1000 Geary St., San Francisco 9, California.
25	Commanding Officer, Office of Naval Research, Navy 100, Fleet Post Office, New York, New York.
6	Director, Naval Research Laboratory, Washington 25, D. C., Attn: Code 2000.
4	Chief, Bureau of Naval Weapons, Department of the Navy, Washington 25, D. C., Attn: 1 - Aero and Hydro Branch 1 - Research Division 2 - Underwater Missile Branch
5	Chief, Bureau of Ships, Department of the Navy, Washington 25, D. C., Attn: 1 - Code 106 1 - Code 310 1 - Code 312 1 - Code 420 1 - Code 554
5	Commanding Officer and Director, David Taylor Model Basin, Washington 7, D. C., Attn: 1 - Code 142 1 - Code 500 1 - Code 513 1 - Code 526 1 - Code 591
1	Commander, U. S. Naval Ordnance Test Station, China Lake, California, Attn: Code 753.
1	Officer-in-Charge, Pasadena Annex, U. S. Naval Ordnance Test Station, 3202 E. Foothill Boulevard, Pasadena, California, Attn: Code P890962.

CopiesOrganization

- 1 Commanding Officer and Director, U. S. Naval Engineering Experiment Station, Annapolis, Maryland.
- 1 Commander, Naval Proving Ground, Dahlgren, Virginia, Attn: Technical Library Division (AAL).
- 1 Commanding Officer, U. S. Naval Underwater Ordnance Station, Newport, Rhode Island, Attn: Research Division.
- 1 Commander, U. S. Naval Ordnance Laboratory, White Oak, Maryland, Attn: Library Division (Desk HL).
- 1 Mr. W. I. Niedermair, Coordinator of Research, Maritime Administration, 441 G Street, N. W., Washington 25, D. C.
- 3 National Bureau of Standards, Washington 25, D. C., Attn:  
 1 - Fluid Mechanics Section  
 1 - Dr. G. B. Schubauer  
 1 - Dr. G. H. Keulegan
- 1 National Academy of Sciences, National Research Council, 2101 Constitution Avenue, N. W., Washington, D. C.
- 1 Superintendent, U. S. Naval Academy, Annapolis, Maryland, Attn: Librarian.
- 1 Superintendent, U. S. Naval Postgraduate School, Monterey, California, Attn: Librarian.
- 1 Superintendent, U. S. Merchant Marine Academy, Kings Point, Long Island, New York, Attn: Captain L. S. McCready, Head, Department of Engineering.
- 1 Air Force Office of Scientific Research, Mechanics Division, Washington 25, D. C.
- 1 Commanding Officer, Office of Ordnance, Box CM, Duke Station, Durham, North Carolina.
- 5 Director of Research, National Aeronautics and Space Agency, 1512 H Street, N. W., Washington 25, D. C.
- 2 Mr. J. B. Parkinson, Langley Aeronautical Laboratory, National Aeronautics and Space Administration, Langley Field, Virginia.
- 1 Director, Engineering Sciences Division, National Science Foundation, 1520 H Street, N. W., Washington, D. C.
- 10 Document Service Center, Armed Services Technical Information Agency, Arlington Hall Station, Arlington 12, Virginia.
- 1 Office of Technical Services, Department of Commerce, Washington 25, D. C.



CopiesOrganization

- 4 California Institute of Technology, Pasadena 4, California, Attn:  
 1 - Professor M. S. Plesset  
 1 - Professor T. Y. Wu  
 1 - Professor A. Acosta  
 1 - Hydro Lab
- 3 University of California, Berkeley 4, California, Attn:  
 1 - Department of Engineering  
 1 - Professor H. A. Schade  
 1 - Professor J. V. Wehausen
- 1 Director, Scripps Institution of Oceanography, University of California, La Jolla, California.
- 1 Professor M. Albertson, Department of Civil Engineering, Colorado State University, Fort Collins, Colorado.
- 2 Iowa Institute of Hydraulic Research, State University of Iowa, Iowa City, Iowa, Attn:  
 1 - Professor H. Rouse, Director  
 1 - Professor L. Landweber
- 2 Harvard University, Cambridge 38, Massachusetts, Attn:  
 1 - Professor G. Birkhoff, Department of Mathematics  
 1 - Professor G. F. Carrier, Division of Engineering and Applied Physics
- 3 Massachusetts Institute of Technology, Cambridge 39, Massachusetts, Attn:  
 1 - Department of N. A. and M. E.  
 1 - Professor A. T. Ippen, Hydro Laboratory  
 1 - Library
- 4 University of Michigan, Ann Arbor, Michigan, Attn:  
 1 - Professor R. B. Couch, Department of N. A. and M. E.  
 1 - Professor C. S. Yih, Department of Engineering Mechanics  
 1 - Professor V. Streeter, Department of Civil Engineering  
 1 - Library
- 1 Director, St. Anthony Falls Hydraulic Laboratory, University of Minnesota, Minneapolis 14, Minnesota.
- 1 Director, Alden Hydraulic Laboratory, Worcester Polytechnic Institute, Worcester, Massachusetts.
- 1 Director, Ordnance Research Laboratory, Pennsylvania State University, University Park, Pennsylvania.
- 1 Director, Institute of Mathematical Sciences, New York University, 25 Waverly Place, New York 3, New York.
- 1 Professor J. J. Foody, Engineering Department, New York State University, Maritime College, Fort Schuyler, New York.

CopiesOrganization

- 1 Technical Library, Webb Institute of Naval Architecture, Crescent Beach Road, Glen Cove, Long Island, New York.
- 1 Professor S. Corrsin, Chairman, Mechanical Engineering Department, The Johns Hopkins University, Baltimore, Maryland.
- 1 Commanding Officer, Office of Naval Research Branch Office, 1030 East Green Street, Pasadena 1, California.
- 1 Director, Woods Hole Oceanographic Institute, Woods Hole, Massachusetts.
- 1 Society of Naval Architects and Marine Engineers, 74 Trinity Place, New York 6, New York.
- 1 Engineering Societies Library, 29 W. 39th Street, New York 18, New York.
- 1 Stevens Institute of Technology, Davidson Laboratories, 711 Hudson Street, Hoboken, New Jersey, Attn:  
 1 - Dr. J. Breslin  
 1 - Mr. D. Savitsky  
 1 - Library
- 1 Director, Institute for Fluid Mechanics and Applied Mathematics, University of Maryland, College Park, Maryland.
- 1 Division of Applied Mathematics, Brown University, Providence 12, Rhode Island.
- 1 Hydrodynamics Laboratory, National Research Council, Ottawa, Canada.
- 1 Professor L. M. Milne-Thomson, Mathematical Research Center, 1118 W. Johnson Center, Madison 6, Wisconsin.
- 1 Dr. J. M. Robertson, Department of Theoretical and Applied Mechanics, College of Engineering, University of Illinois, Urbana, Illinois.
- 2 Stanford University, Stanford, California, Attn:  
 1 - Professor J. K. Venard, Civil Engineering Department  
 1 - Applied Mathematics and Statistics Laboratory
- 1 Professor J. B. Herbich, Civil Engineering Department, Lehigh University, Bethlehem, Pennsylvania.
- 1 Dean J. S. McNown, Department of Engineering Mechanics, University of Kansas, Lawrence, Kansas.
- 1 Professor A. G. Strandhagen, Department of Engineering Mechanics, University of Notre Dame, Notre Dame, Indiana.

CopiesOrganization

- 2 Polytechnic Institute of Brooklyn, Department of Aeronautical Engineering and Applied Mechanics, 333 Jay Street, Brooklyn 1, New York, Attn:  
 1 - Professor A. Ferri  
 1 - Professor H. Reissner
- 1 Professor H. Cohen, IBM Research Center, P. O. Box 218, Yorktown Heights, New York.
- 1 Professor D. Gilbarg, Applied Mathematics and Statistics Laboratory, Stanford University, Stanford, California.
- 1 Mr. Leo Geyer, Chief of Preliminary Design, Grumman Aircraft Engineering Corporation, Bethpage, Long Island, New York.
- 1 Mr. W. P. Carl, Jr., Dynamic Developments, Inc., Babylon, Long Island, New York.
- 1 EDO Corporation, College Point, Long Island, New York.
- 1 Mr. H. E. Brooke, Hydrodynamics Laboratory, Convair, San Diego 12, California.
- 1 Miami Shipbuilding Corporation, 615 S. W. Second Avenue, Miami 36, Florida.
- 1 Baker Manufacturing Company, Evansville, Wisconsin.
- 1 Gibbs and Cox, Inc., 21 West Street, New York 16, New York.
- 1 Dr. H. Reichardt, Max-Planck-Institut fuer Stroemungsforschung, Goettingen, Boettingerstrass 6/8, West Germany,
- 1 Director of Research, National Aeronautics and Space Administration, Lewis Research Center, 21000 Brookpark Road, Cleveland 35, Ohio.
- 2 Hydronautics, Inc., 200 Monroe Street, Rockville, Maryland, Attn:  
 1 - Mr. Phillip Eisenberg  
 1 - Mr. M. P. Tulin
- 1 Commanding Officer and Director, U. S. Naval Civil Engineering Laboratory, Port Hueneme, California, Attn: Code L54.
- 1 Micro-Tech Research Company, 629 Massachusetts Avenue, Cambridge, Massachusetts, Attn: Mr. Cohoon.
- 1 Professor J. E. Cermak, Department of Civil Engineering, Colorado State University, Fort Collins, Colorado.
- 1 Mr. Blaine Parkin, The Rand Corporation, 1700 Main Street, Santa Monica, California.

CopiesOrganization

- |   |   |
|---|---|
| 1 | Cleveland Pneumatic Industry, Inc., Advanced Systems Development Division, 1301 E. El Segundo Boulevard, El Segundo, California.                                |
| 1 | Mr. George H. Pedersen, Turbomachinery Division, Curtiss-Wright Corporation, Research Division, Quehanna, Pennsylvania.   |
| 1 | Dr. Byrne Perry, Department of Civil Engineering, Stanford University, Stanford, California.  |
| 1 | Dr. J. Kotik, Technical Research Group Incorporated, 2 Aerial Way, Syosset, New York.   |
| 1 | Professor H. G. Flynn, Department of Electrical Engineering, The University of Rochester, College of Engineering, River Campus Station, Rochester 20, New York. |
| 1 | Mr. Kenneth E. Hodge, Hydrodynamics Research, Lockheed Aircraft Corporation California Division, Burbank, California.   |